INTERFACE

rsif.royalsocietypublishing.org

Research

Cite this article: Hempel K, Earn DJD. 2015 A century of transitions in New York City's measles dynamics. *J. R. Soc. Interface* **12**: 20150024.
http://dx.doi.org/10.1098/rsif.2015.0024

Received: 8 January 2015
Accepted: 10 March 2015

Subject Areas:
biomathematics

Keywords:
mechanistic modelling, epidemiology, disease ecology, mathematical biology, measles in New York City, disease dynamics

Author for correspondence:
Karsten Hempel
e-mail: hempelkr@math.mcmaster.ca

Electronic supplementary material is available at http://dx.doi.org/10.1098/rsif.2015.0024 or via http://rsif.royalsocietypublishing.org.

THE ROYAL SOCIETY PUBLISHING

A century of transitions in New York City's measles dynamics

Karsten Hempel and David J. D. Earn

Department of Mathematics and Statistics, McMaster University, 1280 Main Street West, Hamilton, Ontario, Canada L8S 4K1

Infectious diseases spreading in a human population occasionally exhibit sudden transitions in their qualitative dynamics. Previous work has successfully predicted such transitions in New York City's historical measles incidence using the seasonally forced susceptible–infectious–recovered (SIR) model. This work relied on a dataset spanning 45 years (1928–1973), which we have extended to 93 years (1891–1984). We identify additional dynamical transitions in the longer dataset and successfully explain them by analysing attractors and transients of the same mechanistic epidemiological model.

1. Introduction

Mechanistic mathematical models are being used increasingly in the study of infectious diseases at the population level and are considered to be powerful tools for predicting epidemiological dynamics [1–3]. Successful modelling of observed epidemic patterns requires access to high-quality data, including disease incidence [4,5] (or disease-induced mortality [6,7]), demography (especially birth rates [8,9]) and changes in contact patterns (e.g. resulting from school vacations [10–12]).

In 1973, London & Yorke [11,12] published monthly measles incidence rates for New York City (NYC) spanning 1928–1973. These data have been extensively studied [4,5,11–15]. We extend the dataset to produce a time series of reported measles cases and concurrent demographic data (total population and total births), which spans the 93 years 1891–1984 (and for much of the incidence time series we increase the temporal resolution from monthly to weekly). Our process of data acquisition, compilation and quality-checking is detailed in §2 and all the data are available in the electronic supplementary material for this paper.[1]

Measles exhibits recurrent epidemics, the frequency and amplitude of which change over long timescales. Much research over the last 40 years has attempted to reveal the biological and dynamical processes that give rise to these changing epidemic patterns, especially the transitions evident in NYC measles dynamics [5,11,14–18]. In this paper, by more than doubling the length of the NYC measles time series, we substantially enhance the opportunity to test hypotheses concerning the mechanisms that drive childhood disease transmission patterns.

We model measles dynamics in NYC using the susceptible–infectious–recovered (SIR) model, which is applicable to diseases for which acquired immunity is permanent [1,2,19]. There has been considerable debate in recent years concerning the most appropriate formulation of the SIR model for childhood infections such as measles [20–26]. We follow Krylova & Earn [6,27], who showed that for measles, the simplest sinusoidally forced SIR model—when suitably parametrized—makes identical predictions to more complicated versions of the model that include realistically distributed latent and infectious periods (details in §3.1).

2. Data compilation

The monthly measles data published by London & Yorke [11,12] span the years 1928–1973. We compiled data of finer temporal resolution (weekly), and extended the time series back to 1891, using a variety of documents stored at the NYC

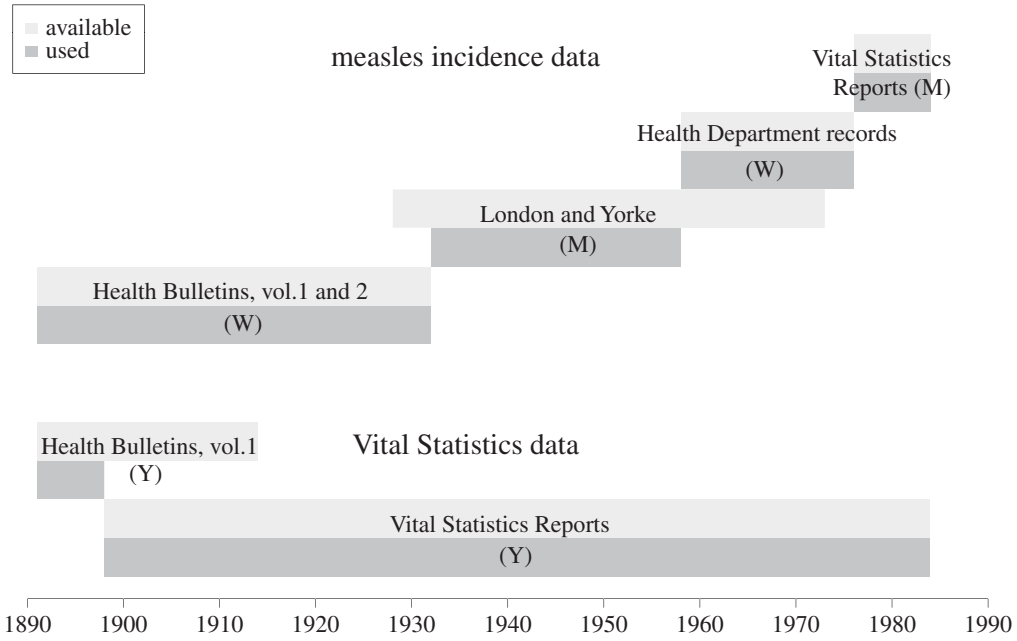

Figure 1. Summary of data available (light grey) and used (dark grey). W, M and Y indicate weekly, monthly and yearly sources, respectively. See electronic supplementary material, §S1 for a detailed description of sources and data compilation.

Academy of Medicine Library.[2] We also extended the monthly measles data forward to 1984 using vital statistics records available on the NYC Health Department website.

Figure 1 summarizes the data sources, including those from which we extracted birth rates. Below we briefly explain some of the issues involved in preparing the full time series for the analyses described in §3. Much greater detail about the data is provided in the electronic supplementary material, §S1.

2.1. Adjustments and normalization

2.1.1. Births

Our data sources typically report vital statistics in NYC as a whole, but the boundary of NYC changed in 1898. Until the end of 1897, NYC included only the island of Manhattan. In January 1898, the city limits were redefined to include The Bronx, Brooklyn, Queens and Richmond. The Vital Statistics Reports are derived from census data and include yearly numbers of total population, births, deaths and infant mortality. We assume these data are reliable, but they extend back only to 1898 [28]. The weekly Health Bulletins include total population estimates and weekly birth counts for Manhattan only, and extend back to 1891. In order to merge these two sets, we aggregate the weekly birth counts yearly, and rescale the birth numbers such that the *per capita* birth rate from 1891 to 1898 meets a linear extrapolation of the *per capita* birth rate from 1898 to 1900. From 1900 to 1935, the Vital Statistics Reports present births and total population numbers only at 5-year intervals, representing the average of yearly values in each interval. For these years, constant values are used over each 5-year interval.

2.1.2. Infant mortality

The Health Bulletins do not contain infant mortality data, and we therefore extrapolate *per capita* infant mortality rates for 1891–1898 from 1898 to 1905 data. Infant mortality was very substantial in the early part of the time series. In 1898, 24% of all reported deaths were infants (in sharp contrast to 2% in 1984).

2.1.3. Measles cases

The NYC Health Department Weekly Bulletins normally reported the city-wide total number of measles cases, but in 1915 measles cases were reported only for three hospitals within the city. We rescaled the aggregated case reports for these three hospitals so that their yearly total matched the reported yearly sum in the 1915 Vital Statistics Report (see the electronic supplementary material, §S1.14 for details).

For most of the period for which we have measles data (1891–1984), we have weekly reports, but we have only monthly incidence for 1932–1958 and 1976–1984. In order to work with a weekly time series for the full length of the dataset, we created weekly time series from the monthly data as follows:

— generate a series of weekly dates that occur on the same day of the week as the dates in the weekly time series segment preceding the monthly data;
— for each new weekly time point, set its measles incidence equal to the number of cases reported for the month within which it falls, divided by the number of weekly points that fall within that month; and
— at this stage, the artificially weekly time series contains four-to-five week blocks of constant incidence. To remove this spurious step-like structure, we smooth the artificial portion of the weekly time series with a 5-point moving average.

Figure 2 shows the resulting weekly measles times series, together with annual births and total population.

2.2. Consistency checks

There is some temporal overlap among the various source documents (figure 1), which facilitates some cross-checking. From 1911 to 1932, we compared the yearly aggregated measles case reports from the Vital Statistics Reports with yearly sums of the data we acquired from the weekly Health Bulletins. From 1928 to 1932, we compared monthly aggregated case

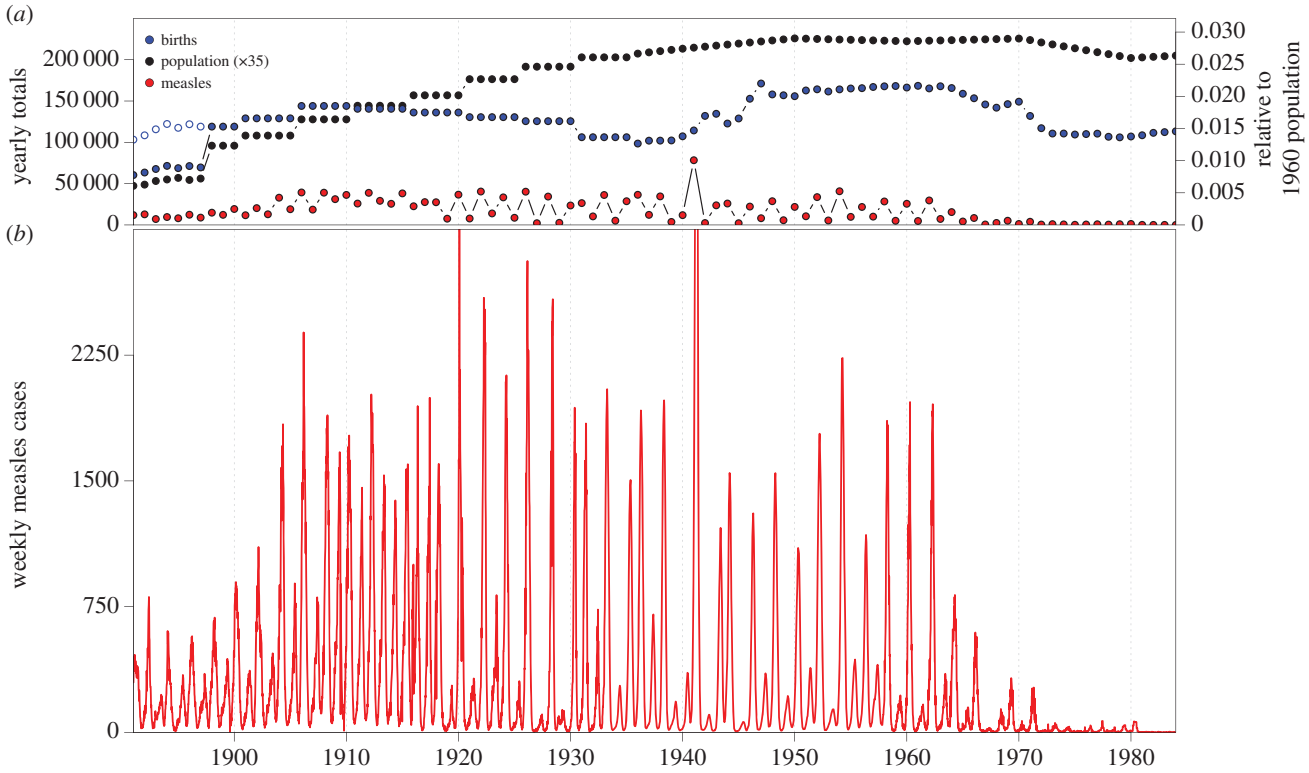

Figure 2. NYC vital statistics and measles case report data, 1891–1984 (for compilation details see §2 and electronic supplementary material, §S1). (*a*) Annual births, estimated total population and reported measles cases. The NYC population was 1 657 000 in 1891 and peaked at 7 903 000 in 1950. Annual births peaked at 171 174 in 1947. Open circles indicate adjusted births, accounting for the change in the boundary of NYC in 1898 (see §2.1). (*b*) Weekly measles cases (as reported, except 1932–1958 and 1976–1984, for which weekly cases were estimated from monthly data; see electronic supplementary material, §S1). Two peaks are cut off in this plot (4671 cases reported for the week ending 31 Jan 1920 and 5016 cases estimated for the week ending 22 Mar 1941). (Online version in colour.)

data from London & Yorke [11] with monthly sums of the weekly reports from the Health Bulletins. Finally, from 1958 to 1973 we compared monthly aggregated case data from London & Yorke [11] with monthly sums of the weekly reports from the Health Department records. In all cases, there is excellent agreement between previously published data and our newly digitized data (see the electronic supplementary material, §S1.8).

3. Analysis

In this section, we describe the tools that we use to examine measles dynamics in NYC. We begin with the SIR model (§3.1), and explain how we use the *effective basic reproduction number* $\mathcal{R}_{0,\mathrm{eff}}$ (§3.2.1) and the estimated *amplitude of seasonal forcing* α (§3.2.2) to predict the periodicity of measles incidence in NYC (§3.3). We estimate $\mathcal{R}_{0,\mathrm{eff}}$ and α as functions of time to generate an SIR-predicted frequency structure for measles in NYC throughout the time period 1891–1984. In §4, we compare the observed frequency structure of the incidence time series (using a continuous wavelet transform) with the SIR-predicted frequency structure.

3.1. The susceptible–infectious–recovered model

The deterministic SIR model [1,19] can be written [27]

$$\frac{\mathrm{d}S}{\mathrm{d}t} = \nu N_0 - \beta SI - \mu S, \tag{3.1a}$$

$$\frac{\mathrm{d}I}{\mathrm{d}t} = \beta SI - \gamma I - \mu I \tag{3.1b}$$

and

$$\frac{\mathrm{d}R}{\mathrm{d}t} = \gamma I - \mu R, \tag{3.1c}$$

where S, I and R denote the numbers of susceptible, infectious and recovered (immune) individuals, respectively. Equations (3.1*a*,*b*) do not depend on the state variable R, so the full dynamics of the system can be described in two dimensions and the third equation can be ignored. The parameters are the rates of transmission (β) and recovery (γ), as well as the *per capita* rates of birth (ν) and death (μ). The mean infectious period is $T_{\mathrm{inf}} = 1/\gamma$. As discussed below, N_0 refers to the population size at a particular 'anchor time' t_0 (as opposed to the current total populations size $N = S + I + R$). We will interpret the 'birth rate' ν more generally as the *per capita* rate of susceptible recruitment (relative to N_0) [2,4,5,13,27]. Here μ represents the *per capita* rate of death from natural causes (disease-induced mortality is assumed to be negligible).

$\mathcal{R}_0$. The *basic reproduction number* $\mathcal{R}_0$ is the average number of secondary cases caused by a primary case in a wholly susceptible population [1,29]. If births balance deaths, then for the SIR model $\mathcal{R}_0 = \beta N/(\gamma + \mu)$ [1]. In our situation (3.1), typically $\nu \neq \mu$ and [27]

$$\mathcal{R}_0 = \frac{\nu N_0}{\mu}\frac{\beta}{\gamma+\mu}. \tag{3.2}$$

We assume that the susceptible recruitment rate ν changes slowly enough that $\mathcal{R}_0$ can be defined at a given time by treating ν as a constant. Secular changes in ν can induce dynamical transitions [2,4,5,13,27], as we discuss in §3.3.

3.1.1. Seasonality

To account for seasonally varying transmission arising from aggregation of children in schools [2,5,11,15], we assume

Table 1. Demographic and disease parameter estimates for NYC.

parameter	meaning	estimate	source
fixed parameters			
γ^{-1}	mean generation time	13 days	[1,27]
μ	natural death rate	0.02 yr^{-1}	[5]
N_0	population in 1960	7 782 000	[28]
ν_0	births in 1960 /N_0	0.0214	[28]
$\mathcal{R}_0$	basic reproduction number in 1960	17	[1,4,5]
parameter	**meaning**	**range**	**source**
time-varying parameters			
B	births per year	98 507 – 171 174	[28]
D_{infant}	infant deaths per year	1540 – 16 609	[28]
p	proportion vaccinated	0 – 0.66	[33]
ν	susceptible recruitment per year	0.00473 – 0.0214	equation (3.4); §3.2.1
$\mathcal{R}_{0,\text{eff}}$	effective $\mathcal{R}_0$	3.86 – 17.5	equation (3.5); §3.2.1
α	amplitude of seasonal forcing	0.11 – 0.21	equation (3.3); §3.2.2

the transmission rate is seasonally forced,

$$\beta(t) = \beta_0(1 + \alpha\cos(2\pi t)), \tag{3.3}$$

where β_0 is the mean transmission rate, α is the amplitude of forcing and time t is measured in years. We use the simple sinusoidal forcing function (3.3) rather than more realistic term-time forcing [5,17] because the two yield virtually identical dynamics (for different α values) [5,27]. Introducing time-dependence into the transmission rate generally affects the basic reproduction number $\mathcal{R}_0$ [30,31]; however, for the SIR model (3.1), inserting the mean transmission rate β_0 in place of β in equation (3.2) is correct [32].

3.1.2. Susceptible – infectious – recovered versus susceptible – exposed – infectious – recovered

Most previous work on measles dynamics has been based on the SEIR model (e.g. [4,5,14,15]), which includes an additional class (E) of *exposed* individuals who are infected but not yet infectious. Because the mean latent period for measles ($T_{\text{lat}} \simeq 8$ days, [1]) is long relative to the mean infectious period ($T_{\text{inf}} \simeq 5$ days, [1]), it is natural to assume that the SEIR model will represent measles dynamics better than the simpler SIR model, which includes no latent period. However, Krylova & Earn [27] showed that the SIR model displays virtually identical dynamics to the SEIR if the length of the mean generation interval (≃13 days) is used for the mean infectious period in the SIR model. This dynamical correspondence holds also for versions of the SIR and SEIR model with realistically distributed stage durations, rather than the exponential distributions implied by equation (3.1) [27]. We therefore use the SIR model (3.1) with $T_{\text{inf}} = 13$ days.

3.2. Parameter estimates

Table 1 summarizes our estimated parameter values. There are two categories of parameters, those that are assumed to be fixed and those that vary in time. Our analysis in §3.3 involves predicting the dynamical effects of changes in $\mathcal{R}_{0,\text{eff}}$ (which depends on changes in susceptible recruitment ν through births B and proportion vaccinated p, §3.2.1) and changes in the amplitude of seasonal forcing α.

Following previous work [4,5,27], we estimate $\mathcal{R}_0$ in 1960 by assuming the standard estimate for England and Wales in 1960 [1, p. 70] also applies to NYC. Susceptible recruitment in 1960, ν_0, arises entirely from births because the measles vaccine was not yet available and immigration of *susceptibles* into NYC was negligible (most immigrants would have been immune).

Note that the natural death rate indicated in table 1 yields a mean lifetime $\mu^{-1} = 50$ years, which is much shorter than the true mean lifetime. This intentional discrepancy accounts partially for the long tail in the implicitly assumed exponential distribution of lifetimes. Our results are insensitive to the value of μ because most people contract measles as children, and immune individuals do not affect transmission.

3.2.1. Effective basic reproduction number $\mathcal{R}_{0,\text{eff}}$

Because our estimate of $\mathcal{R}_0$ (equation (3.2)) is for 1960, we take our 'anchor time' to be $t_0 = 1960$. Susceptible recruitment (ν) is defined in terms of births (B), infant mortality (D_{infant}), the population size at the anchor time (N_0) and vaccine uptake (p),

$$\nu(t) = \frac{B(t) - D_{\text{infant}}(t)}{N_0}(1 - p(t)). \tag{3.4}$$

Infant mortality is deducted here because it represents a large reduction in new susceptibles early in the NYC time series (see §2.1). The effective $\mathcal{R}_0$ is [2,5,27]

$$\mathcal{R}_{0,\text{eff}}(t) = \frac{\nu(t)N_0}{\mu}\frac{\beta_0}{\gamma+\mu} = \frac{\nu(t)}{\nu_0}\mathcal{R}_0. \tag{3.5}$$

Thus, the time series $\mathcal{R}_{0,\text{eff}}(t)$ is strictly proportional to $\nu(t)$ (figure 3).

3.2.2. Seasonal forcing amplitude

We estimate the seasonal forcing amplitude α as a function of time using the method of Krylova [6, ch. 4]. Krylova improved on the earlier method of Fine & Clarkson [34] for estimating $\beta(t)$ by allowing for reporting delays, accounting for natural mortality, and removing the restriction that the

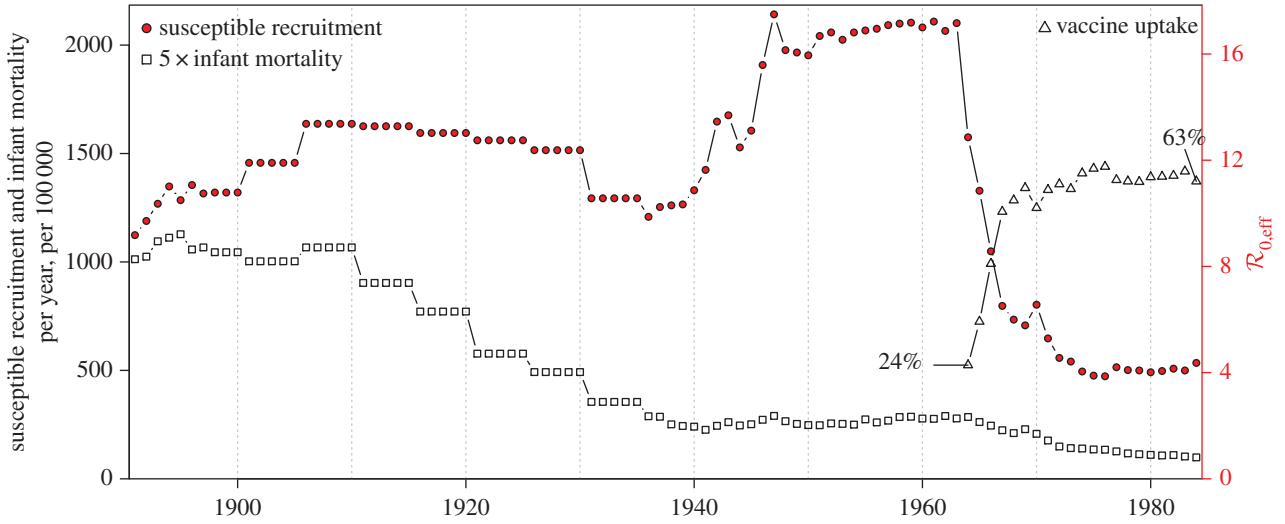

Figure 3. Susceptible recruitment $\nu(t)$ in NYC, as defined by equation (3.4). From the scaling given in equation (3.5), the effective basic reproduction number $\mathcal{R}_{0,\mathrm{eff}}(t)$ is proportional to $\nu(t)$ and its value is indicated on the right axis. Annual infant mortality (scaled by five for clarity) and estimated annual vaccine uptake (since 1964) are also shown. (Online version in colour.)

generation interval must be equal to the observation interval, requiring instead that the generation interval is an integer multiple of the observation interval.

Krylova's method [28, ch. 4] begins by reconstructing the time series of the number of susceptible individuals in the population via

$$S_{t+\Delta t} = S_t + (1 - p_t)B_t - \frac{1}{\rho_t} C_{t+\Delta t+T_{\mathrm{report}}} - \frac{D_t}{P_t} S_t . \tag{3.6}$$

The symbols here refer, for the time interval from t to $t + \Delta t$, to the number of susceptibles (S_t), the proportion of newborns vaccinated (p_t), the number of births (B_t, adjusted for infant mortality), the proportion of cases reported (ρ_t), the number of cases reported (C_t), the number of deaths from natural causes (D_t) and the total population size (P_t). The time interval between reports is Δt (one week in our case) and the average reporting delay is T_{report} (taken to be two weeks). Following Fine & Clarkson [34], we infer the reporting efficiency ρ_t by assuming that all surviving individuals eventually contract measles (hence we estimate ρ_t as a moving average of measles cases divided by a moving average of susceptible recruitment).

As in the Fine & Clarkson [34] algorithm, an estimate of the proportion of the population susceptible is required at a single time point. We assumed that at time $t = 1900$ this proportion was $S_0/P_0 = 0.05$, which is near the endemic equilibrium of the unforced SIR model [1]. Our results are not sensitive to the precise value of S_0 assumed. A bad guess leads to an obvious spurious trend in the reconstructed susceptible time series. See Krylova [6, p. 134] and deJonge [35, p. 16] for greater detail on this issue.

After reconstructing the full time series of susceptibles $\{S_t\}$, the transmission rate at time t is estimated via [6, eqn 4.12]

$$\beta_t = \frac{1}{S_t} \frac{C_{t+T_{\mathrm{report}}}}{C_{t+T_{\mathrm{report}}-T}} (\gamma + \mu_t). \tag{3.7}$$

Krylova's method requires that the disease generation interval be an integer multiple of the observation interval. The mean generation interval for measles $\gamma^{-1} = 13$ days, and following [6,34] we approximate this as $T = 2$ weeks (table 1).

Given the full time series $\{\beta_t\}$, the seasonal pattern for a given year y containing reporting dates t_i, $i = 1, \ldots, 52$, can be expressed

$$\beta^y_{t_i} = \frac{\beta_{t_i} - \langle \beta_{t_i} \rangle}{\langle \beta_{t_i} \rangle}, \tag{3.8}$$

where angle brackets refer to the average over the 52 reporting dates in year y. The underlying pattern of seasonality should not vary substantially from year to year (since population contact structures do not change significantly from year to year). To reduce the noise in the inferred seasonality, $\beta^y_{t_i}$, we obtain the median seasonal pattern over a 9 year period centred on the focal year y. Thus, we replace each $\beta^y_{t_i}$ with

$$\tilde{\beta}^y_{t_i} = \mathrm{Median}\{\beta^{y+j}_{t_i}\}^4_{j=-4} . \tag{3.9}$$

The estimated seasonal pattern (3.9) is our observational equivalent of the term $\alpha \cos 2\pi t$ in the sinusoidally forced transmission rate (3.3) that we use in the SIR model (3.1). However, in order to use the sinusoidally forced SIR model to make predictions, we must estimate the amplitude (α) of sinusoidal forcing to which the observed forcing pattern (3.9) is equivalent. Previous work [5] has indicated that such an equivalence does exist and can be found by matching stable or unstable period doubling bifurcation points—along the main branch of the $\mathcal{R}_0$ bifurcation diagram—that occur when forcing the SIR model with a sinusoidal versus observed seasonal pattern; the match is accomplished by making a sequence of $\mathcal{R}_0$ bifurcation diagrams with different sinusoidal forcing amplitudes (α) until an α value is found that yields a bifurcation diagram in which the focal bifurcation occurs at the same $\mathcal{R}_0$ value as in the bifurcation diagram made with the observed seasonal forcing pattern. We separately matched stable and unstable period doubling bifurcations and found negligible difference in the estimated α. We also varied the averaging window from 5 to 13 years and found no significant differences from the 9 year window specified above. In order to quantify uncertainty in one α estimate, we computed 25% and 75% quartiles of the seasonal pattern in (3.9) along with the median. For these quartiles, we matched the stable and unstable period doubling bifurcations, as we did for the median. Our estimated α time series is shown in figure 4.

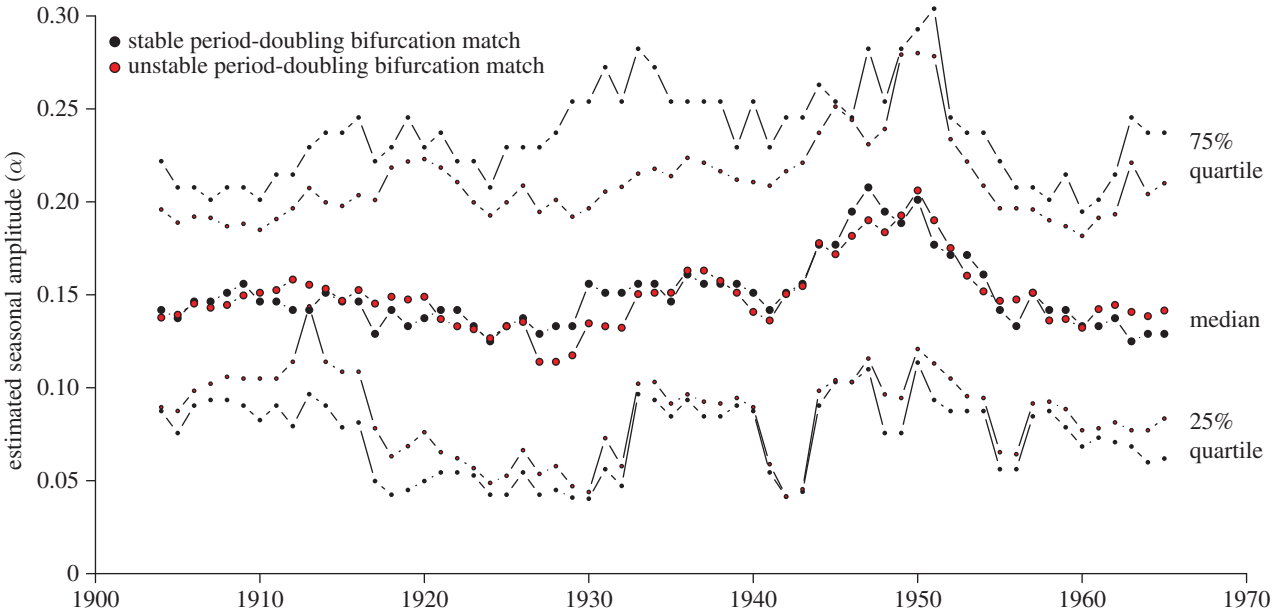

Figure 4. Estimates of the amplitude (α) of seasonality of measles transmission, from 1904 to 1965, based on 9-year time windows around each year (details in §3.2.2). The measles incidence data after 1970 (after mass vaccination was in full force) is much noisier and estimating α is much more difficult. We assume α remained roughly constant after the final point shown in the graph. (Online version in colour.)

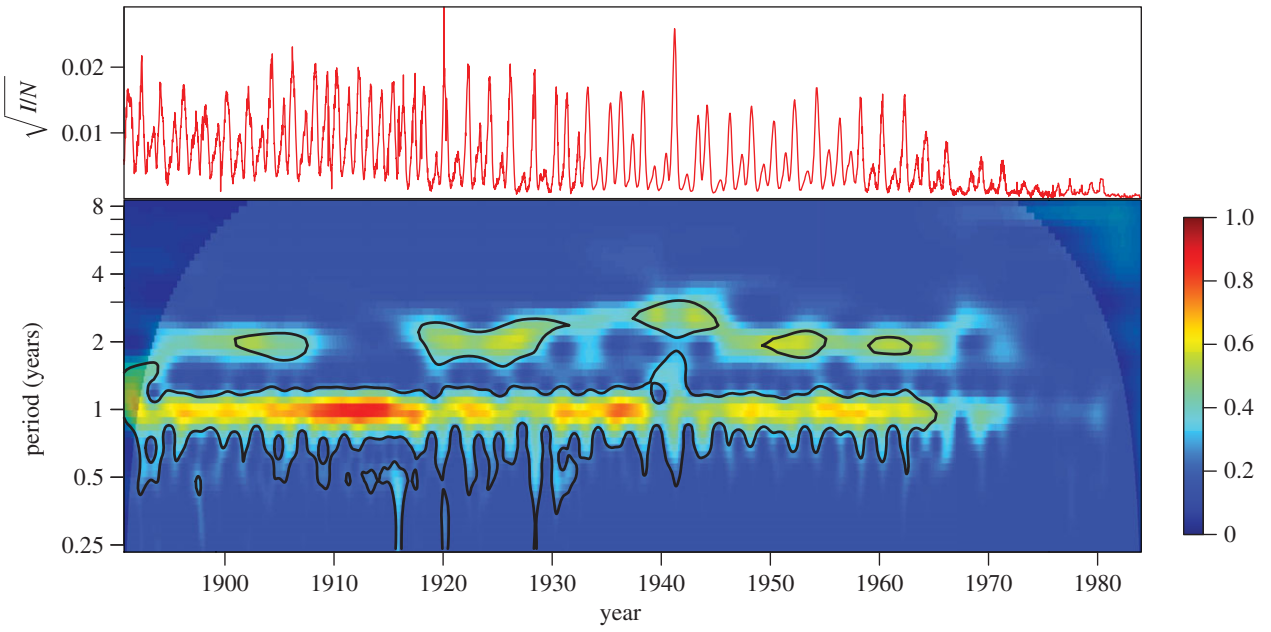

Figure 5. Observed measles dynamics in NYC from 1891 to 1984. (*a*) Square root of measles case reports, normalized by total concurrent population. (*b*) Colour depth plot of a continuous wavelet transform of the square root of normalized observed NYC measles cases (colour warmth scales with spectral power and 95% significance contours are shown in black). Shaded regions in the upper left and right indicate the cone of influence [36]. (Online version in colour.)

We estimate α only from 1900 to 1970. We avoid pre-1900 data due to the previously mentioned change in reporting area in 1898 (§2), and lack of data outside Manhattan. We do not produce estimates beyond 1970 because case sampling is worse, resulting in poor and unreliable reconstruction. Since we use 9-year windows to produce estimates, and data from 1900 to 1970, we produce α estimates for the years 1904–1965. The temporal progressions of both our predictor parameters ($\mathcal{R}_{0,\mathrm{eff}}$ and α) are shown in a figure in §3.3.3 for the full time series.

3.3. Transition analysis

Previous work has shown that analysis of the deterministic SIR model (3.1) is sufficient to predict changes in the frequency structure of observed temporal patterns of infectious disease incidence [2,4,5,27] or mortality [6] observed over many decades. The methodology has been described in detail previously [27, §2.2]. Here we briefly summarize our analysis as we apply it to the newly extended NYC measles times series, emphasizing the aspects of our approach that differ from previous transition analyses.

3.3.1. Features of the data that we would like to explain

Figure 2 presented all the data used for our analyses. Figure 5 displays the normalized NYC measles time series again, but in two different ways that highlight the changes in frequency structure that we seek to understand. The top panel of figure 5 shows weekly normalized measles on a square root scale, suppressing

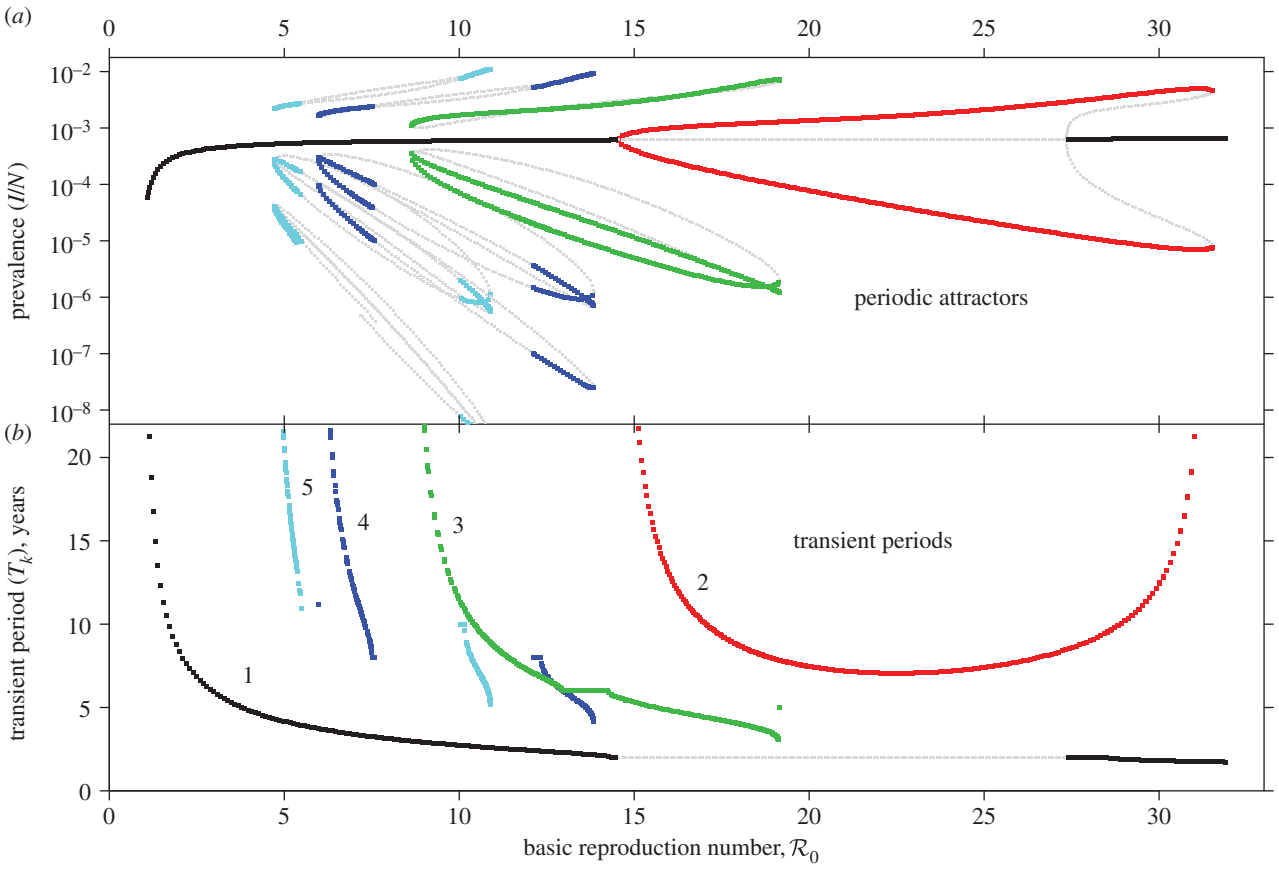

Figure 6. Attractor analysis diagram for measles parametrized for NYC, constructed using XPPAUT [42]. This figure is similar to Krylova [6, fig. 9], but the seasonal amplitude here is $\alpha = 0.12$ rather than $\alpha = 0.08$. (*a*) For each value of $\mathcal{R}_0$ on the *x*-axis, yearly values of the *infected* SIR compartment are shown (on a log-scale) from long-term solutions of the system (ignoring transient dynamics). The light grey lines show repellers, which can have important influences on dynamics [43]. Parameter values used are $\mu = \nu = 0.02\ \mathrm{yr}^{-1}$, $\alpha = 0.12$, $\gamma = (365/13)/\mathrm{yr} \simeq 28.1\ \mathrm{yr}^{-1}$. Longer period attractors exist for this parametrization of the SIR model, but their basins of attraction are small and they have not been observed in real-world systems. Our analysis is focused on the main branch, which shows, from left to right, a stable period doubling and an unstable period doubling bifurcation. (*b*) Transient periods associated with each of the attractors displayed in (*a*), computed as in [4,27]. (Online version in colour.)

epidemic magnitude in favour of exposing periodic structure. The bottom panel of the figure shows the corresponding continuous wavelet transform [36–40], which reveals the dominant frequencies at each point in time.

The main features of the wavelet transform in figure 5 are two spectral peaks at almost all times. Throughout most of the time series, there is a peak at a period of 1 year. The period of the second peak varies between 2 and 3 years (and is absent from about 1912 to 1915). *Can we explain the existence and spectral position of these peaks over the course of the time series?*

3.3.2. Attractor and transient periods as functions of $\mathcal{R}_0$

For any given parameter set and initial conditions, the solution of the SIR model (3.1) yields predicted dynamics that can be compared with the observed time series. In particular, two periods can usually be extracted from (non-chaotic) SIR solutions: (i) the period of the attractor that is reached asymptotically and (ii) the period of the transient during approach to the attractor. The *attractor period*—or resonant period—of the SIR model is always an integer multiple of the 1-year forcing period and is typically inferred from bifurcation diagrams of the stroboscopic map associated with the model [5]. The *transient period*—or non-resonant period—can be a time of any length and is obtained by a linear perturbation analysis of the associated attractor [4]. (For an attractor with period k, its transient period T_k is given by $2\pi k/|\mathrm{Arg}(\lambda_k)|$, where λ_k is the dominant eigenvalue of the associated stroboscopic map [4,13].) Both resonant and non-resonant periods are expected to be observed in real incidence time series because demographic stochasticity sustains transient dynamics [4,41].

Naively, there are many model parameters (β, γ, ν, μ, N_0, α) and possible initial conditions (S_0, I_0) to consider when attempting to make predictions using the SIR model (3.1). However, the relationship between susceptible recruitment and effective reproduction number (equation (3.5)) can be exploited [2,4,5,27] to reduce the relevant number of parameters to one: predictions can be made from the SIR model (3.1) by considering only how periodicity of solutions varies as a function of the basic reproduction number $\mathcal{R}_0$ (equation (3.2)) with all other parameters fixed (provided the amplitude of seasonality α can be taken to be constant throughout the observed time series).

Figure 6 presents predicted NYC measles dynamics as a function of $\mathcal{R}_0$. The top panel is a bifurcation diagram for the SIR model (3.1) and the bottom panel shows the transient

periods associated with each attractor. From these diagrams, we can read off the predicted attractor and transient period for any given $\mathcal{R}_0$. For $\mathcal{R}_0$ values for which multiple attractors coexist, predicted dynamics are history-dependent and demographic stochasticity can lead to switching among attractors [5,44]; however, in real incidence time series we are unlikely to detect attractors with periods other than 1 or 2 years, for a number of reasons:

(i) attractors with periods longer than 2 years typically have small attracting basins,
(ii) long-period attractors typically have unrealistically low prevalence levels,
(iii) brief excursions of long-period attractors will not be distinguishable from noise and
(iv) in the presence of noise, some long-period attractors are indistinguishable from lower period attractors.

The predicted transient periods for non-annual attractors are all very long; in practice, only the transient period associated with the annual attractor is likely to be observable. The degree of spectral power generated by a transient varies with the system's proximity to the associated attractor. During time intervals when the system is very close to the attractor, the transient period can be undetectable (we demonstrate this effect through stochastic simulations in the electronic supplementary material, §S2).

3.3.3. Attractor periods as functions of both $\mathcal{R}_0$ and α

For the era (1928–1972) of NYC measles dynamics that has been studied previously [4,5,11,27], it was reasonable to assume that the amplitude of seasonal forcing (α) was roughly constant. With our much longer time series going back to 1890, this approximation is less likely to be valid. We therefore estimated the amplitude of *time-varying* seasonality in §3.2.2. To make use of estimates of both $\mathcal{R}_{0,\mathrm{eff}}(t)$ and $\alpha(t)$, we need a two-dimensional equivalent of figure 6, showing how attractors and transients vary as functions of both $\mathcal{R}_0$ and α.

Figure 7 presents a two-dimensional bifurcation diagram for the SIR model (3.1), which shows the regions of the ($\mathcal{R}_0$, α) parameter plane in which attractors of various lengths exist. The black curve shows the estimated trajectory of NYC measles in this parameter plane (based on the median value of α shown in figure 4). The boxed region is shown on a larger scale in figure 8, and the last two digits of many years are marked along the ($\mathcal{R}_0(t)$, $\alpha(t)$) curve.

4. Results

We summarize our results in figure 9. As in figure 5, figure 9*a*,*c* shows the NYC measles incidence time series and wavelet spectrum, which we aim to explain using the SIR model (equation (3.1)).

Figure 9*b* shows predicted attractor periods for each year from 1891 to 1984. For each year, the SIR model was solved for 10 000 distinct initial states and the period of the attractor to which the solution converged was recorded. The coloured bands show the proportion of runs that converged onto an attractor of the period indicated in the legend; thus the relative lengths of the coloured bands can be viewed as estimates of the relative volumes of the basins of attraction associated with each periodic attractor. The collection of initial states for a given year (t) was chosen as follows:

— the initial proportion susceptible (S_0) was varied from 80% to 120% of the proportion that would be susceptible at equilibrium ($1/\mathcal{R}_{0,\mathrm{eff}}(t)$) if the system were unforced;
— the initial prevalence (I_0) was varied throughout the range of observed weekly incidence (before 1963 for the pre-vaccine era and after 1963 for the vaccine era);
— a 100×100 grid of initial states was considered in the region of the (S_0, I_0) plane specified above. For each grid point, the model parameters were set according to table 1, except that the estimated $\mathcal{R}_{0,\mathrm{eff}}(t)$ (figure 3) was used in place of $\mathcal{R}_0$, and the seasonal amplitude (α) was chosen at random from a uniform distribution between the lower and upper quartile of the estimated $\alpha(t)$ (figure 4) for the year in question.

In years for which multiple attractors are predicted, any of these attractors could occur in a particular realization of the underlying stochastic process. In each year, we take the predicted attractor period to be that of the attractor to which the greatest number of simulations converged. Black circles indicate these attractors on the wavelet spectrum. White vertical bars identify the possible ranges of transient periods associated with these attractors (an annual attractor for most of the time series, but a biennial attractor from 1946 to 1963). The heavy white dot on the white bars indicates the median transient period for the simulations associated with the given year.

The qualitative agreement between predicted and observed spectral peaks in figure 9 is very good. In greater detail

1891–1945

Observed behaviour: the wavelet spectrum has a substantial peak at a period of 1 year throughout this time interval, and a secondary peak near a period of 2 years is evident except during 1909–1917. From 1909 to 1917, the incidence time series shows very similar annual epidemics.

Predicted periods: panel *b* shows that an annual attractor exists throughout this year range with a larger estimated basin of attraction than other attractors. Other longer period attractors with smaller estimated basins of attraction coexist with the annual for some years (also see figure 8, white circles). The median predicted transient period varies between 2.20 and 2.58 years over this time span and is slightly longer than the observed (2 year) secondary peak period before about 1905.

Interpretation: since the wavelet spectrum does not show power near period 3 at the beginning of the time series (excluding information inside the cone of influence), we conclude that the real system was near the period 1 attractor initially. The system appears to remain near the period 1 attractor for the duration of this time interval, which can be explained by the consistently high volume of attraction of the annual attractor. Where they exist, longer period coexisting attractors might influence the dynamics, but their effects would likely be indistinguishable from noise because the temporal segments in question are too short for multiple cycles of these longer period attractors to be completed. The power near period 2 throughout this time interval is always close to the predicted transient period

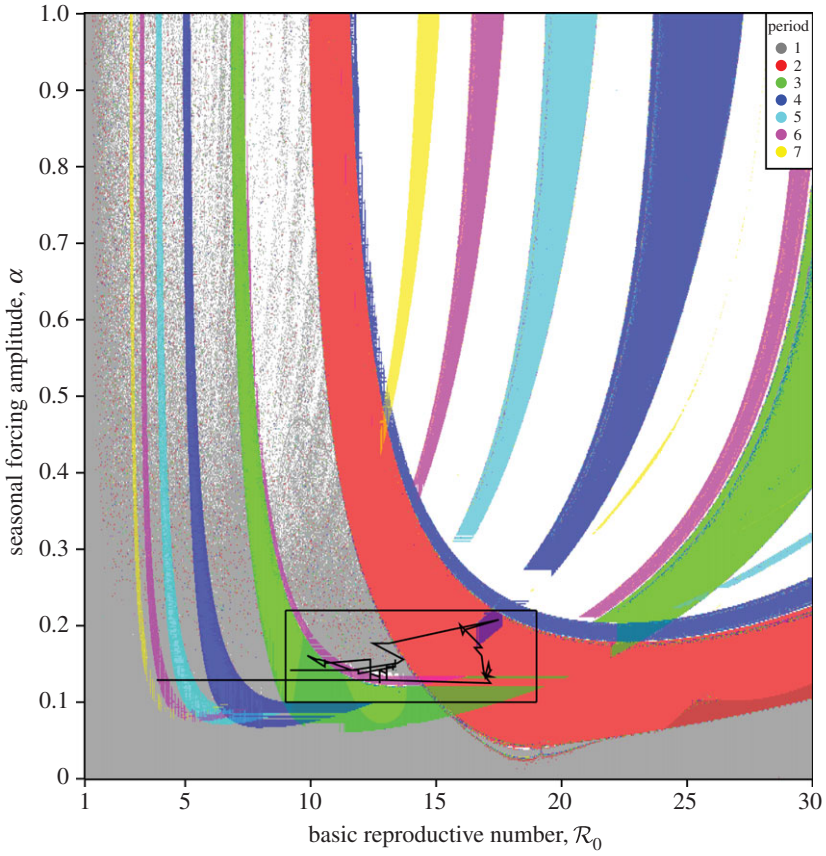

Figure 7. Periodic attractors in the sinusoidally forced SIR model (§3.1) as a function of basic reproduction number $\mathcal{R}_0$ and seasonal amplitude α ($\mu = \nu = 0.02\ \mathrm{yr}^{-1}$, $\gamma = 28.1\ \mathrm{yr}^{-1}$). The black curve shows the trajectory of NYC measles in this parameter plane, based on our estimates of $\mathcal{R}_{0,\mathrm{eff}}$ and α for the period 1891–1984. The colour of each point represents the period (in years) of the attractor to which the SIR system has converged. Partial colour transparency allows us to display the existence of multiple attractors for given $\mathcal{R}_0$ and α. A systematic exploration of the full range of initial conditions for each parameter pair ($\mathcal{R}_0$, α) was not computationally feasible, but we integrated the model from the initial state variables $S_0 = 10^{-1}$ and $I_0 = 10^{-3}$. We computed the grid by row from left to right, right to left, and by column from top to bottom, and bottom to top. In each case, after the initial point on a row or column, we use the final conditions of the simulation for one point as the initial conditions for the next. Results from all four grid computations are overlaid. White regions on the plot indicate either periods longer than shown in the legend or lack of simulation convergence to any periodic attractor.

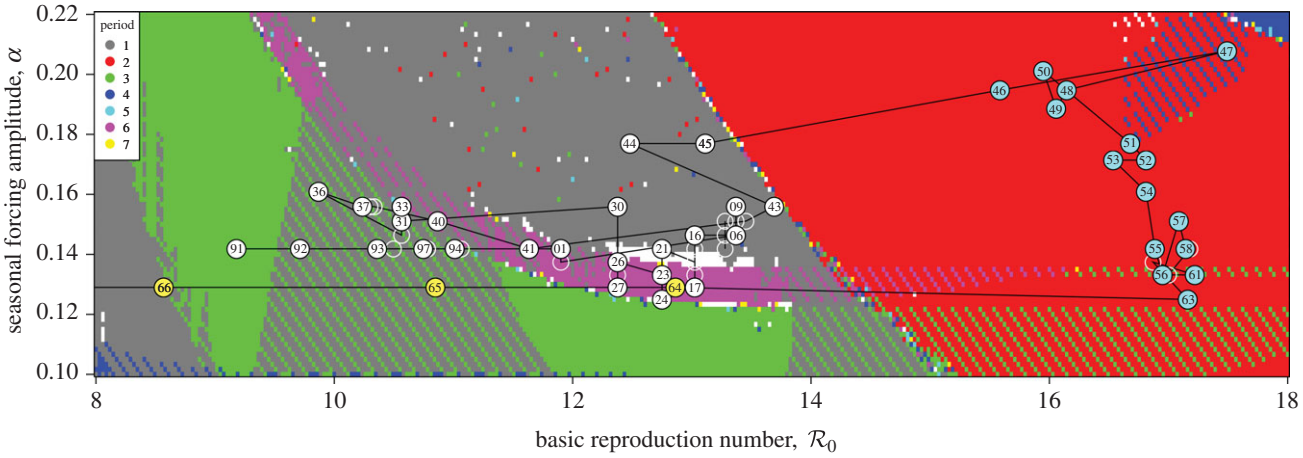

Figure 8. Zoomed-in and enhanced version of the boxed region in figure 7. The estimated yearly parameter time series ($\mathcal{R}_{0,\mathrm{eff}}(t)$, $\alpha(t)$) is overlaid on the colour-coded attractor plot. Different epochs have been marked with different coloured circles; 1891–1945 white, 1946–1963 teal and 1964–1984 yellow. The number in each circle is the last two digits of year t for t in the range 1891–1984 (some years are marked with white circles and no year for readability). Where more than one resonant period is possible (depending on initial conditions), coexistence of multiple attractors is shown with alternating stripes.

associated with the period 1 attractor. The power observed at a transient period in an infectious disease time series varies significantly, as stochasticity affects the proximity of the system to the periodic attractor. The temporary absence of power near period 2 is a phenomenon that we have reproduced with the estimated parameter values using stochastic simulations (electronic supplementary material, §S2).

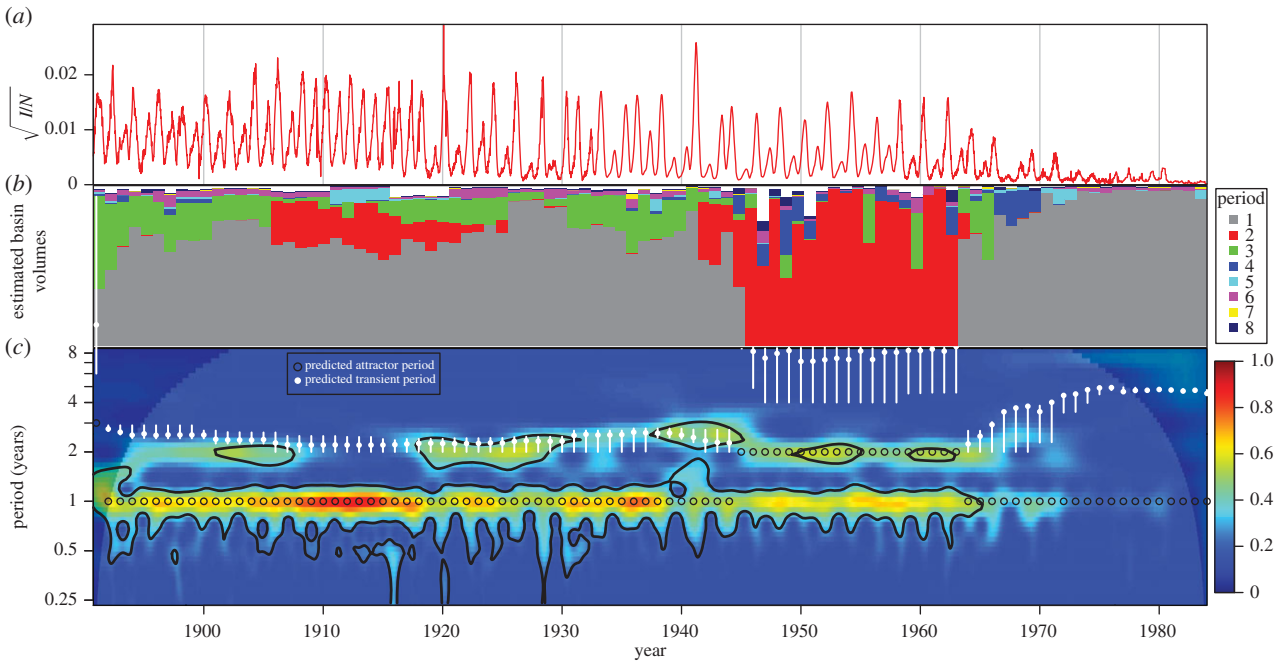

Figure 9. Comparison of predicted versus observed measles dynamics in NYC from 1891 to 1984. (*a*) Square root of measles case reports, normalized by total concurrent population. (*b*) Approximate volumes of basins of attraction near the observed NYC measles incidence for each year from 1891 to 1984. For each year, we display the proportion of 10 000 simulations that reach each period. See §4 for details. (*c*) Colour depth plot of a continuous wavelet transform of the square root of normalized observed NYC measles cases (colour warmth scales with spectral power and 95% significance contours are shown in black). The predicted attractor and transient periods are overlaid (only the periods of annual and biennial attractor transients are short enough to appear on this graph and to be observable). Unfilled black circles indicate predicted attractor periods that are consistent with the observed data.

1946–1963

Observed behaviour: there is substantial power at precisely periods 1 and 2 years throughout this time interval.

Predicted periods: the greatest estimated basin volume throughout this interval is occupied by a period 2 attractor, with coexisting longer period attractors also present (also see figure 8, teal circles).

Interpretation: the multi-year attractors that are identified always display power at a 1-year period in addition to the period of the attractor because the multi-year epidemic pattern involves epidemics every year. Since a biennial attractor is the most probable throughout this time interval, we expect to see the observed power at 1 and 2 years.

1964–1984

Observed behaviour: the wavelet diagram shows power near period 1 year throughout the time interval, and power near periods 2 and 3 years up to 1973. The time series appears very noisy and a dramatic drop in incidence is evident beginning in 1965.

Predicted periods: an annual attractor exists throughout this time interval, with sporadically coexisting attractors of periods 3–6 years. No biennial attractor is predicted (also see figure 8, yellow circles).

Interpretation: vaccination was introduced in NYC in 1963, accounting for the dramatic drop in cases. As cases drop, dynamics are governed more by demographic and extrinsic stochasticity than periodic attractors. This accounts for the weakness of spectral peaks. We conclude that the system transitioned from a biennial attractor to an annual attractor near the beginning of this time interval, which is consistent with predicted behaviour. The weak spectral peak at period 1 year until 1980 suggests that the system remained near the annual attractor until the end of the time series.

5. Discussion

The NYC measles incidence data published in 1973 by London & Yorke [11,12] has inspired a great deal of research on infectious disease dynamics [2,4,11,14,15]. Given the impact of the London and Yorke time series (monthly reported measles cases from 1928 to 1972), we were motivated to extend the dataset to more than twice its previous length (1891–1984), and in so doing we obtained long spans of higher quality (weekly rather than monthly) data. To complement the measles data, we compiled annual birth and population data for NYC for same year range. We collected data from a number of distinct sources, which contained some overlapping years, allowing us to perform sanity checks and either verify data quality or make minor corrections.

Previous work [4,5,27] has used mechanistic epidemic models to understand transitions in measles dynamics in NYC from 1928 to 1972. These analyses made predictions of dynamical transitions based on changes in the effective basic reproduction number $\mathcal{R}_{0,\mathrm{eff}}$ (estimated from changes in susceptible recruitment arising from births and vaccination), and a fixed amplitude of seasonal forcing (α). For our analysis of transitions in the newly extended time series, we generalized this approach to allow for changes in both $\mathcal{R}_{0,\mathrm{eff}}$ and α and estimated both over the course of the observed time series.

There is excellent agreement between our SIR model predictions of dominant periods and the observed frequency structure in the data quantified by a continuous wavelet

transform (figure 9). All observed transitions can be explained using the deterministic SIR model by a combination of changes in birth rate, vaccination and the effect of demographic stochasticity preventing transient oscillations from damping out [41,45].

We did not, in this paper, attempt to predict the relative magnitudes of the observed spectral peaks in the NYC measles wavelet spectrum. Doing so requires analysis of the stochastic SIR model, either by simulation [2,4] or by analytical or semi-analytical methods that have begun to be applied to infectious disease dynamics in recent years [16,46].

We did point out an unusual feature of the new earlier segment of the NYC measles time series from 1909 to 1917, namely the complete lack of spectral power at any period other than 1 year, even though an observable transient period near 2 years is predicted. As a proof of principle, we showed in electronic supplementary material, §S2 that precisely this behaviour can be reproduced in stochastic SIR simulations, but we did not quantify the probability of such behaviour occurring. One possible direction for future work would be to examine the wavelet spectra of large numbers of realizations of the stochastic SIR model with the parameters estimated for NYC measles (including the vaccine era during which demographic stochasticity plays a much larger role); analysing such a collection of simulations would allow us to estimate the probability distribution of relative transient power at each point along the time series, and more generally the probability of observing a time series very similar to the real data. This would be computationally expensive, but seems likely to be enlightening and could substantially enhance our understanding of dynamical transitions in recurrent patterns of infectious disease epidemics.

Acknowledgements. We could not have carried out this research without the indispensable cooperation of the New York Academy of Medicine Library, where most of the new data were found. We are particularly grateful to Arlene Shaner (Reference Librarian and Acting Curator, Rare Books and Manuscripts). We thank Ben Bolker, David Champredon, Jonathan Dushoff, Chai Molina, Irena Papst, and Dora Rosati for helpful comments and discussions.

Funding statement. We were supported by an Ontario Graduate Scholarship (K.H.) and the Natural Sciences and Engineering Research Council of Canada (D.J.D.E.).

Endnotes

[1]The data compiled for this paper are also available from the International Infectious Disease Data Archive (IIDDA) at http://iidda.mcmaster.ca.

[2]The NYC Academy of Medicine (www.nyam.org) is a public institution independent of the NYC Health Department. Its library maintains a collection of books and literature related to health in the NYC population throughout its history.

References

1. Anderson RM, May RM. 1991 *Infectious diseases of humans: dynamics and control*. Oxford, UK: Oxford University Press.
2. Earn DJD. 2009 Mathematical epidemiology of infectious diseases. In *Mathematical biology*, vol. 14 (eds MA Lewis, MAJ Chaplain, JP Keener, PK Maini), pp. 151–186. IAS/Park City Mathematics Series. Providence, RI: American Mathematical Society.
3. Hethcote HW. 2000 The mathematics of infectious diseases. *SIAM Rev.* **42**, 599–653. (doi:10.1137/S0036144500371907)
4. Bauch CT, Earn DJD. 2003 Transients and attractors in epidemics. *Proc. R. Soc. Lond. B* **270**, 1573–1578. (doi:10.1098/rspb.2003.2410)
5. Earn DJD, Rohani P, Bolker BM, Grenfell BT. 2000 A simple model for complex dynamical transitions in epidemics. *Science* **287**, 667–670. (doi:10.1126/science.287.5453.667)
6. Krylova O. 2011 Predicting epidemiological transitions in infectious disease dynamics: smallpox in historic London (1664–1930). PhD thesis, McMaster University, Canada.
7. Tien JH, Poinar HN, Fisman DN, Earn DJD. 2011 Herald waves of cholera in nineteenth century London. *J. R. Soc. Interface* **8**, 756–760. (doi:10.1098/rsif.2010.0494)
8. He D, Earn DJD. 2007 Epidemiological effects of seasonal oscillations in birth rates. *Theoret. Popul. Biol.* **72**, 274–291. (doi:10.1016/j.tpb.2007.04.004)
9. Martinez-Bakker M, Bakker KM, King AA, Rohani P. 2014 Human birth seasonality: latitudinal gradient and interplay with childhood disease dynamics. *Proc. R. Soc. B* **281**, 20132438. (doi:10.1098/rspb.2013.2438)
10. Earn DJD, He D, Loeb MB, Fonseca K, Lee BE, Dushoff J. 2012 Effects of school closure on incidence of pandemic influenza in Alberta, Canada. *Ann. Intern. Med.* **156**, 173–181. (doi:10.7326/0003-4819-156-3-201202070-00005)
11. London W, Yorke JA. 1973 Recurrent outbreaks of measles, chickenpox and mumps. I. Seasonal variation in contact rates. *Am. J. Epidemiol.* **98**, 453–468.
12. Yorke JA, London W. 1973 Recurrent outbreaks of measles, chickenpox and mumps. II. Systematic differences in contact rates and stochastic effects. *Am. J. Epidemiol.* **98**, 468–482.
13. Bauch CT, Earn DJD. 2003 Interepidemic intervals in forced and unforced SEIR models. In *Dynamical systems and their applications in biology*, vol. 36 (eds S Ruan, G Wolkowicz, J Wu), of *Fields Institute Communications*, pp. 33–44. Toronto, Canada: American Mathematical Society.
14. Bolker BM, Grenfell BT. 1993 Chaos and biological complexity in measles dynamics. *Proc. R. Soc. Lond. B* **251**, 75–81. (doi:10.1098/rspb.1993.0011)
15. Olsen LF, Schaffer WM. 1990 Chaos versus noisy periodicity: alternative hypotheses for childhood epidemics. *Science* **249**, 499–504. (doi:10.1126/science.2382131)
16. Alonso D, McKane AJ, Pascual M. 2007 Stochastic amplification in epidemics. *J. R. Soc. Interface* **4**, 575–582. (doi:10.1098/rsif.2006.0192)
17. Schenzle D. 1984 An age-structured model of pre- and post-vaccination measles transmission. *IMA J. Math. Appl. Med. Biol.* **1**, 169–191. (doi:10.1093/imammb/1.2.169)
18. Stone L, Olinky R, Huppert A. 2007 Seasonal dynamics of recurrent epidemics. *Nature* **446**, 533–536. (doi:10.1038/nature05638)
19. Kermack WO, McKendrick AG. 1927 A contribution to the mathematical theory of epidemics. *Proc. R. Soc. Lond. A* **115**, 700–721. (doi:10.1098/rspa.1927.0118)
20. Black AJ, McKane AJ. 2010 Stochasticity in staged models of epidemics: quantifying the dynamics of whooping cough. *J. R. Soc. Interface* **7**, 1219–1227. (doi:10.1098/rsif.2009.0514)
21. Conlan AJK, Rohani P, Lloyd AL, Keeling M, Grenfell BT. 2010 Resolving the impact of waiting time distributions on the persistence of measles. *J. R. Soc. Interface* **7**, 623–640. (doi:10.1098/rsif.2009.0284)
22. Keeling MJ, Grenfell BT. 2002 Understanding the persistence of measles: reconciling theory, simulation and observation. *Proc. R. Soc. Lond. B* **269**, 335–343. (doi:10.1098/rspb.2001.1898)
23. Lloyd AL. 2001 Destabilization of epidemic models with the inclusion of realistic distributions of infectious periods. *Proc. R. Soc. Lond. B* **268**, 985–993. (doi:10.1098/rspb.2001.1599)
24. Lloyd AL. 2001 Realistic distributions of infectious periods in epidemic models: changing patterns of persistence and dynamics. *Theoret. Popul. Biol.* **60**, 59–71. (doi:10.1006/tpbi.2001.1525)
25. Nguyen HTH, Rohani P. 2008 Noise, nonlinearity and seasonality: the epidemics of whooping cough

revisited. *J. R. Soc. Interface* **5**, 403–413. (doi:10.1098/rsif.2007.1168)

26. Wearing HJ, Rohani P, Keeling MJ. 2005 Appropriate models for the management of infectious diseases. *PLoS Med.* **2**, e320. (doi:10.1371/journal.pmed.0020320)
27. Krylova O, Earn DJD. 2013 Effects of the infectious period distribution on predicted transitions in childhood disease dynamics. *J. R. Soc. Interface* **10**, 20130098. (doi:10.1098/rsif.2013.0098)
28. New York City Department of Health and Mental Hygiene, Office of Vital Records. *Summary of Vital Statistics, 1961–2007 Archived Reports*. http://www.nyc.gov/html/doh/html/vr/vrarchives.shtml.
29. van den Driessche P, Watmough J. 2002 Reproduction numbers and sub-threshold endemic equilibria for compartmental models of disease transmission. *Math. Biosci.* **180**, 29–48. (doi:10.1016/S0025-5564(02)00108-6)
30. Bacaer N. 2009 Periodic matrix population models: growth rate, basic reproduction number, and entropy. *Bull. Math. Biol.* **71**, 1781–1792. (doi:10.1007/s11538-009-9426-6)
31. Bacaer N, Gomes MGM. 2009 On the final size of epidemics with seasonality. *Bull. Math. Biol.* **71**, 1954–1966. (doi:10.1007/s11538-009-9433-7)
32. Ma J, Ma Z. 2006 Epidemic threshold conditions for seasonally forced SEIR models. *Math. Biosci. Eng.* **3**, 161–172. (doi:10.3934/mbe.2006.3.161)
33. Simpson DM, Ezzati-Rice TM, Zell ER. 2001 Forty years and four surveys: how does our measuring measure up? *Am. J. Prev. Med.* **20**, 6–14. (doi:10.1016/S0749-3797(01)00286-0)
34. Fine PEM, Clarkson JA. 1982 Measles in England and Wales—I: an analysis of factors underlying seasonal patterns. *Int. J. Epidemiol.* **11**, 5–14. (doi:10.1093/ije/11.1.5)
35. deJonge MS. 2014 Fast estimation of time-varying transmission rates for infectious diseases. MSc thesis, McMaster University, Canada.
36. Torrence C, Compo GP. 1998 A practical guide to wavelet analysis. *Bull. Am. Meteorol. Soc.* **79**, 61–78. (doi:10.1175/1520-0477(1998)079<0061:APGTWA>2.0.CO;2)
37. Cazelles B, Chavez M, de Magny GC, Guegan JF, Hales S. 2007 Time-dependent spectral analysis of epidemiological time-series with wavelets. *J. R. Soc. Interface* **4**, 625–636. (doi:10.1098/rsif.2007.0212)
38. Cazelles B, Chavez M, Berteaux D, Ménard F, Vik JO, Jenouvrier S, Stenseth NC. 2008 Wavelet analysis of ecological time series. *Oecologia* **156**, 287–304. (doi:10.1007/s00442-008-0993-2)
39. Holdsworth AM, Kevlahan NKR, Earn DJD. 2012 Multifractal signatures of infectious diseases. *J. R. Soc. Interface* **9**, 2167–2180. (doi:10.1098/rsif.2011.0886)
40. Johansson MA, Cummings DAT, Glass GE. 2009 Multiyear climate variability and dengue—El Niño southern oscillation, weather, and dengue incidence in Puerto Rico, Mexico, and Thailand: a longitudinal data analysis. *PLoS Med.* **6**, e1000168. (doi:10.1371/journal.pmed.1000168)
41. Baxendale PH, Greenwood PE. 2011 Sustained oscillations for density dependent Markov processes. *J. Math. Biol.* **63**, 433–457. (doi:10.1007/s00285-010-0376-2)
42. Ermentrout B. 2002 *Simulating, analyzing, and animating dynamical systems: a guide to XPPAUT for researchers and students*. Philadelphia, PA: Software, Environments, and Tools. Society for Industrial and Applied Mathematics.
43. Rand DA, Wilson HB. 1991 Chaotic stochasticity: a ubiquitous source of unpredictability in epidemics. *Proc. R. Soc. Lond. B* **246**, 179–184. (doi:10.1098/rspb.1991.0142)
44. Schwartz IB. 1985 Multiple stable recurrent outbreaks and predictability in seasonally forced nonlinear epidemics. *J. Math. Biol.* **21**, 347–361. (doi:10.1007/BF00276232)
45. Bartlett MS. 1957 Measles periodicity and community size. *J. R. Stat. Soc. Series A* **120**, 48–70. (doi:10.2307/2342553)
46. Black AJ, McKane AJ. 2010 Stochastic amplification in an epidemic model with seasonal forcing. *J. Theor. Biol.* **267**, 85–94. (doi:10.1016/j.jtbi.2010.08.014)

A Century of Transitions in New York City's Measles Dynamics
Electronic Supplementary Material

Journal of the Royal Society Interface (2015)

Karsten Hempel and David J.D. Earn
Department of Mathematics & Statistics, McMaster University,
1280 Main Street West, Hamilton, Ontario, Canada, L8S 4K1

March 28, 2015

Contents

S1 The Data

Two data files that we compiled accompany this paper and can be downloaded from the web site of the *Journal of the Royal Society Interface* or from the International Infectious Disease Data Archive (IIDDA, http://iidda.mcmaster.ca).

`meas_us_ny_nyc_1890-1984_wk.csv`
: Weekly measles cases in New York City (NYC).

`vital_us_ny_nyc_1890-1984_yr.csv`
: Annual vital statistics in NYC (population, births, deaths, infant mortality, proportion vaccinated).

These datasets span 4 October 1890 to 30 December 1983, and were pieced together from four different sources.

S1.1 The Health Dept. Bulletins: 1891–1932 Weekly Data

Near the end of the 19th century and in the first half of the 20th, the NYC Health Department published weekly bulletins containing information regarding a wide variety of public health related issues (see §S3 for sample photographs of such a bulletin). Some of the details provided in these bulletins were incidence rates for numerous infectious diseases, including measles. Spanning the years 1891–1932, the weekly bulletins were published in two volumes. We acquired access to these through the NYC Academy of Medicine Library [1]

As noted previously, vital statistics for the whole of NYC were acquired through the NYC Health Dept., which provides data going back to 1900 [2]. However, we require data going back to the beginning of measles incidence data in 1891. To fill in the missing years of 1891–1899, we extracted vital statistics from the health bulletins.

An important note must be made about these bulletins regarding their reporting area. The data tables in the bulletins provide data for only Manhattan Island up until 15 January 1898, after which the reporting area was enlarged to cover Manhattan, The Bronx, Brooklyn, Queens, and Richmond. We wish to retain as high consistency as possible between the reporting area of both measles incidence data and vital statistics. It is therefore advantageous to use disease incidence data and vital statistics from the same source, especially through a change in reporting area.

S1.1.1 Disease Incidence, Volume 1: 1891–1914

City-wide reported cases of measles were extracted from a table as shown in Figure S1.

[1] The NYC Academy of Medicine [1] is a public institution independent of the NYC Health Department. Its library maintains a collection of books and literature related to health in the NYC population throughout its history.

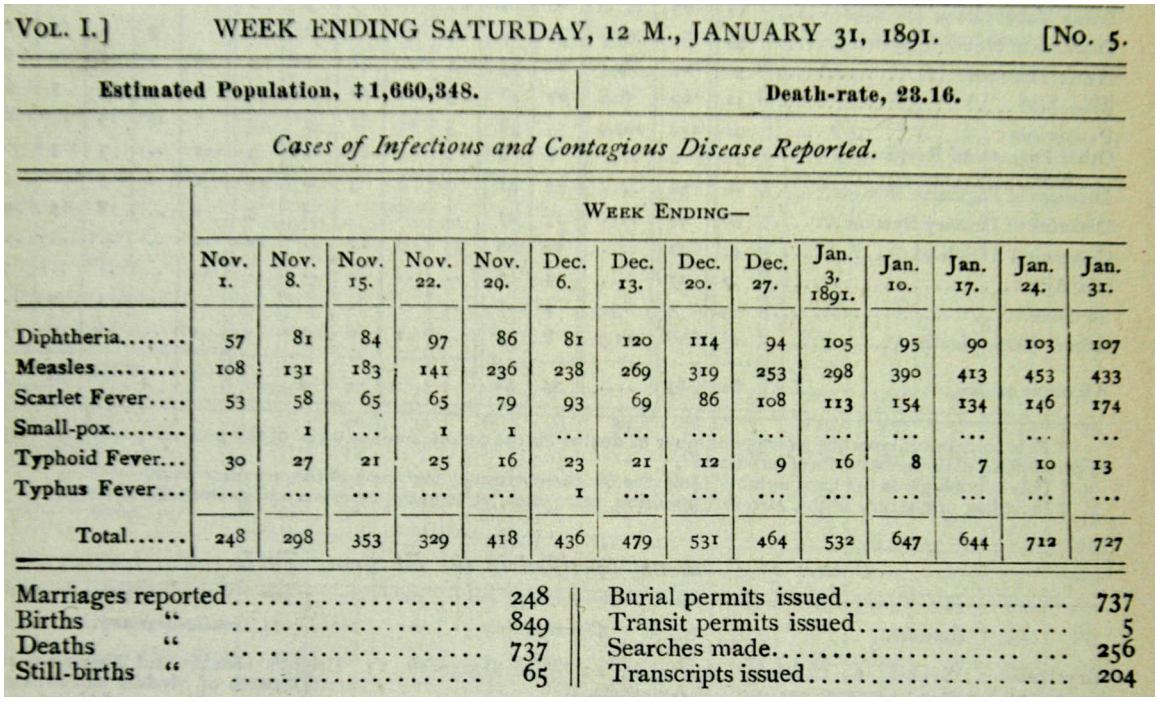

VOL. I.] WEEK ENDING SATURDAY, 12 M., JANUARY 31, 1891. [NO. 5.

Estimated Population, ‡1,660,348. | **Death-rate, 23.16.**

Cases of Infectious and Contagious Disease Reported.

	WEEK ENDING—													
	Nov. 1.	Nov. 8.	Nov. 15.	Nov. 22.	Nov. 29.	Dec. 6.	Dec. 13.	Dec. 20.	Dec. 27.	Jan. 3, 1891.	Jan. 10.	Jan. 17.	Jan. 24.	Jan. 31.
Diphtheria.....	57	81	84	97	86	81	120	114	94	105	95	90	103	107
Measles.....	108	131	183	141	236	238	269	319	253	298	390	413	453	433
Scarlet Fever....	53	58	65	65	79	93	69	86	108	113	154	134	146	174
Small-pox.....	...	1	...	1	1	...	...	...	...	...	...	...	...	...
Typhoid Fever...	30	27	21	25	16	23	21	12	9	16	8	7	10	13
Typhus Fever...	...	...	...	...	...	1	...	...	...	...	...	...	...	...
Total.....	248	298	353	329	418	436	479	531	464	532	647	644	712	727

Marriages reported	248	Burial permits issued	737
Births "	849	Transit permits issued	5
Deaths "	737	Searches made	256
Still-births "	65	Transcripts issued	204

Figure S1: Health Bulletin table reporting weekly cases of infectious diseases. See §S3 for full page.

S1.1.2 Vital Statistics, Volume 1: 1890–1899

Tables of the form shown in Figure S1 in volume 1 of the bulletins provide needed vital data where it could otherwise not be found.

S1.1.3 Vital Statistics, Volume 1: 1898 Change in Reporting Area

The bulletin published for the week of Jan 15, 1898 was the first to include the larger reporting area mentioned previously. Vital statistics tables for that week and the one prior are shown in Figure S2 and Figure S3 to demonstrate the transition. Notice that though these consecutive bulletins occur in the same volume, their format changes to include data from the different boroughs.

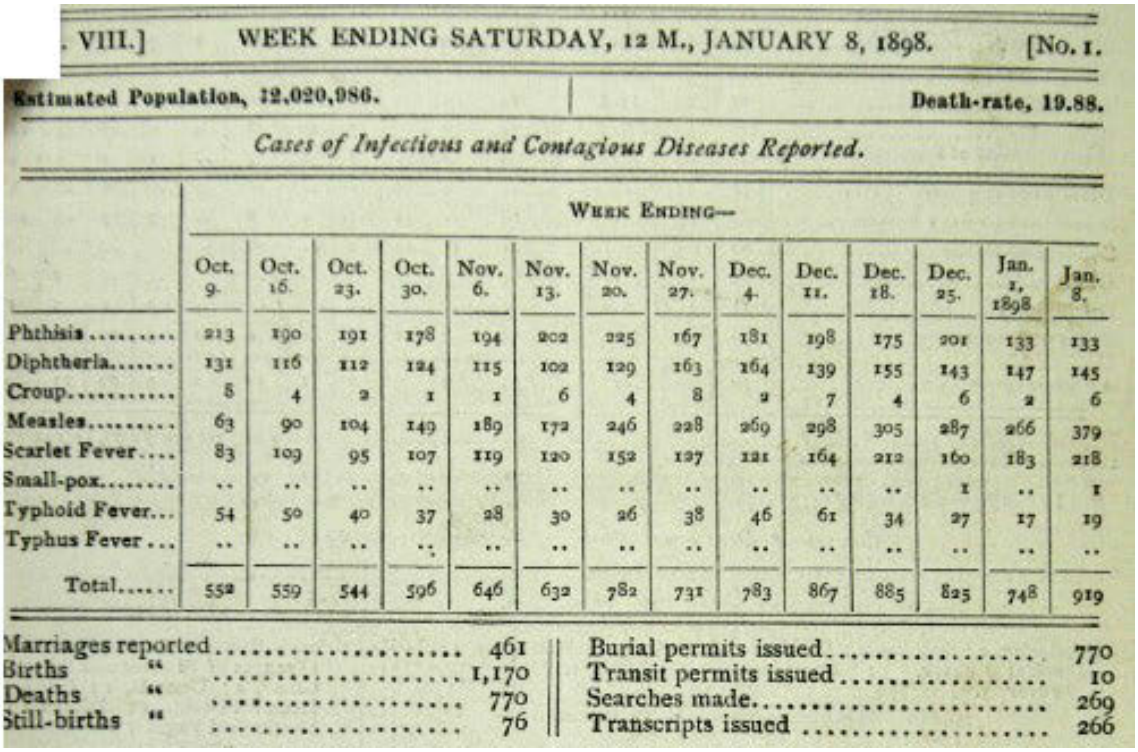

. VIII.] WEEK ENDING SATURDAY, 12 M., JANUARY 8, 1898. [No. 1.

Estimated Population, 12,020,986. **Death-rate, 19.88.**

Cases of Infectious and Contagious Diseases Reported.

	Week Ending—												
	Oct. 9.	Oct. 16.	Oct. 23.	Oct. 30.	Nov. 6.	Nov. 13.	Nov. 20.	Nov. 27.	Dec. 4.	Dec. 11.	Dec. 18.	Dec. 25.	Jan. 1, 1898	Jan. 8.
Phthisis	213	190	191	178	194	202	225	167	181	198	175	201	133	133
Diphtheria	131	116	112	124	115	102	129	163	164	139	155	143	147	145
Croup	8	4	2	1	1	6	4	8	2	7	4	6	2	6
Measles	63	90	104	149	189	172	246	228	269	298	305	287	266	379
Scarlet Fever	83	109	95	107	119	120	152	127	121	164	212	160	183	218
Small-pox	..	..	..	..	..	..	..	..	..	..	..	1	..	1
Typhoid Fever	54	50	40	37	28	30	26	38	46	61	34	27	17	19
Typhus Fever	..	..	..	..	..	..	..	..	..	..	..	..	..	..
Total	552	559	544	596	646	632	782	731	783	867	885	825	748	919

Marriages reported	461	Burial permits issued	770
Births "	1,170	Transit permits issued	10
Deaths "	770	Searches made	269
Still-births "	76	Transcripts issued	266

Figure S2: Health Bulletin table reporting vital statistics for only Manhattan Island, week of Jan. 8, 1898.

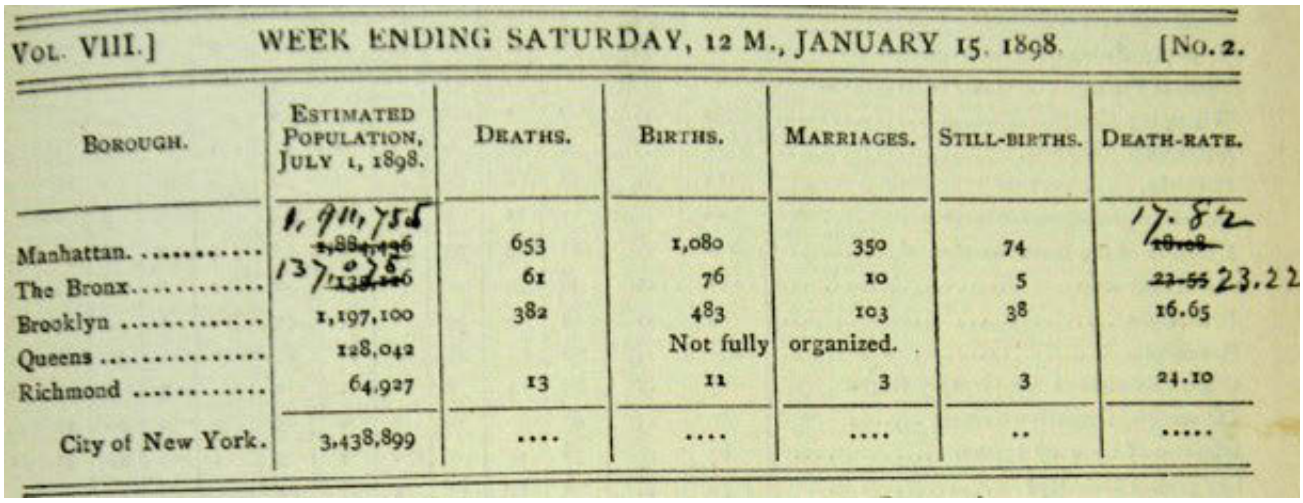

VOL. VIII.] WEEK ENDING SATURDAY, 12 M., JANUARY 15, 1898. [No. 2.

Borough.	Estimated Population, July 1, 1898.	Deaths.	Births.	Marriages.	Still-births.	Death-rate.
Manhattan	1,911,756 ~~1,884,496~~	653	1,080	350	74	17.82 ~~18.08~~
The Bronx	137,025 ~~138,106~~	61	76	10	5	~~23.55~~ 23.22
Brooklyn	1,197,100	382	483	103	38	16.65
Queens	128,042		Not fully	organized.		
Richmond	64,927	13	11	3	3	24.10
City of New York.	3,438,899	....	....	....	..	.....

Figure S3: Health Bulletin table reporting vital statistics for Manhattan, The Bronx, Brooklyn, Queens, and Richmond, week of Jan 15, 1898. The handwritten corrections are uncommon in these documents; they are the result of Health Dept. reorganization.

S1.1.4 Disease Incidence: 1915

Sometime between 1914 and 1916, the NYC Health Dept. adjusted the form of its bulletins, and the transitional year, 1915, presents some difficulty. Figure S4 shows the only available data tables regarding cases of reportable infectious diseases found for that year.

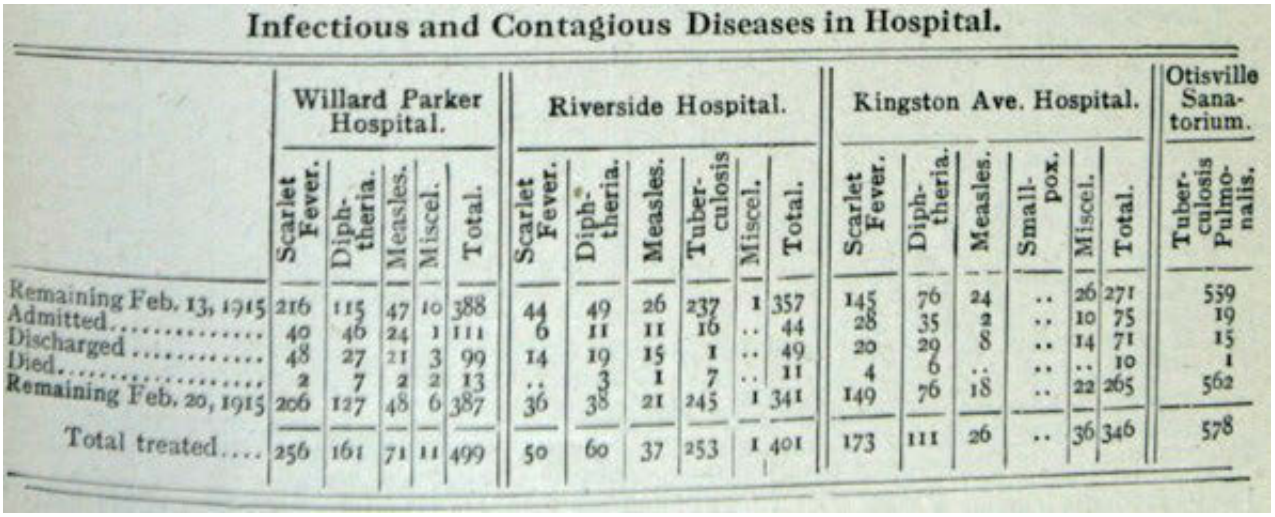

Infectious and Contagious Diseases in Hospital.

	Willard Parker Hospital.					Riverside Hospital.						Kingston Ave. Hospital.						Otisville Sanatorium.
	Scarlet Fever.	Diphtheria.	Measles.	Miscel.	Total.	Scarlet Fever.	Diphtheria.	Measles.	Tuberculosis	Miscel.	Total.	Scarlet Fever.	Diphtheria.	Measles.	Smallpox.	Miscel.	Total.	Tuberculosis Pulmonalis.
Remaining Feb. 13, 1915	216	115	47	10	388	44	49	26	237	1	357	145	76	24	..	26	271	559
Admitted	40	46	24	1	111	6	11	11	16	..	44	28	35	2	..	10	75	19
Discharged	48	27	21	3	99	14	19	15	1	..	49	20	29	8	..	14	71	15
Died	2	7	2	2	13	..	3	1	7	..	11	4	6	..	..	..	10	1
Remaining Feb. 20, 1915	206	127	48	6	387	36	38	21	245	1	341	149	76	18	..	22	265	562
Total treated	256	161	71	11	499	50	60	37	253	1	401	173	111	26	..	36	346	578

Figure S4: Health Bulletin table showing reportable infectious diseases, week of Feb. 20, 1915. See §S3 for full page.

Notice that city-wide totals of cases are not reported. Instead measles cases are reported only for three hospitals within the city. These numbers are themselves not representative of the entire city, but fortunately we can re-scale them using an independent data source (see §S1.4).

S1.1.5 Disease Incidence, Volume 2: 1916–1932

The format of the tables from which disease incidence data were drawn changed slightly compared to the previous volume, and tables appeared as shown in Figure S5.

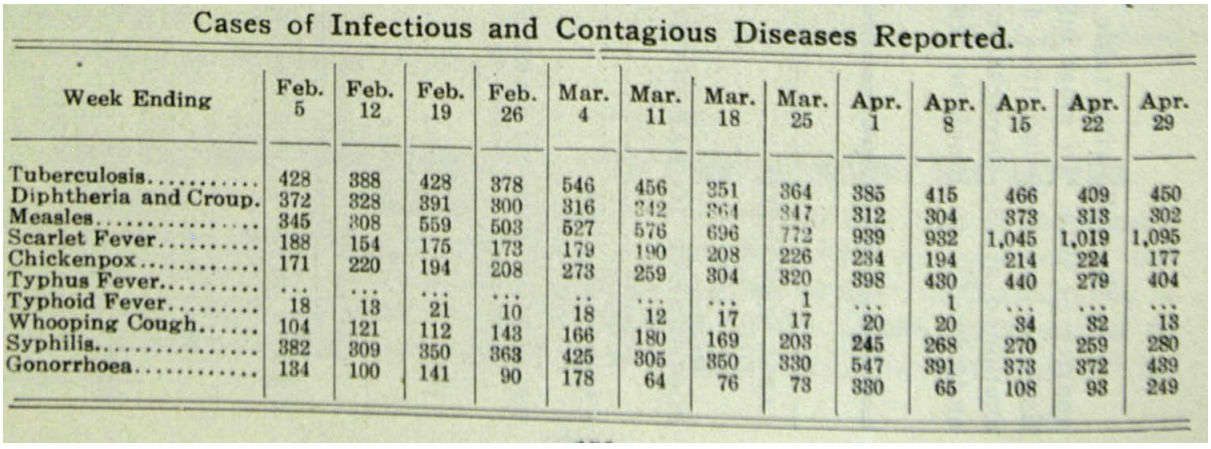

Cases of Infectious and Contagious Diseases Reported.

Week Ending	Feb. 5	Feb. 12	Feb. 19	Feb. 26	Mar. 4	Mar. 11	Mar. 18	Mar. 25	Apr. 1	Apr. 8	Apr. 15	Apr. 22	Apr. 29
Tuberculosis	428	388	428	378	546	456	351	364	385	415	466	409	450
Diphtheria and Croup.	372	328	391	300	316	242	264	347	312	304	373	313	302
Measles	345	308	559	503	527	576	696	772	939	932	1,045	1,019	1,095
Scarlet Fever	188	154	175	173	179	190	208	226	234	194	214	224	177
Chickenpox	171	220	194	208	273	259	304	320	398	430	440	279	404
Typhus Fever	...	...	...	...	..	...	...	1	...	1	...	...	...
Typhoid Fever	18	13	21	10	18	12	17	17	20	20	34	32	18
Whooping Cough	104	121	112	143	166	180	169	203	245	268	270	259	280
Syphilis	382	309	350	363	425	305	350	330	547	391	373	372	439
Gonorrhoea	134	100	141	90	178	64	76	73	330	65	108	93	249

Figure S5: Health Bulletin table reporting weekly cases of infectious diseases. See §S3 for full page.

S1.1.6 Tabulation

For the tables containing disease incidence rates in volumes 1 and 2, notice that for each week's bulletin, a full quarter-year of previous weeks' worth of reported cases are shown. This means that in order to extract a year's worth of data, no more than five sample bulletins are required. As a result, we did not photograph

all Weekly Bulletin pages, but instead sampled pages periodically such that completely overlapping disease incidence tables were acquired.

Notice that the table providing vital statistics shows only information for the week in question. For the total population of NYC at the time, this did not present a problem; weekly changes in population are not significant compared to the total population, we can therefore estimate a yearly average population from these numbers. Birth rates oscillate throughout the year [8], and so for years in which a full set of bulletin photographs had not been acquired, we use weekly data points available periodically throughout the year to estimate the yearly value.

S1.2 Health Dept. Records 1958–1976 Weekly Disease Incidence Data

The NYC Health Department kept detailed records of the incidence of many diseases and conditions, including infectious diseases of interest to us. In particular, from 1958–1976, weekly records were kept of the incidence of diseases and conditions by health district of residence, of which there are 27 in NYC (this date range represents only what we were able to find, but all indications suggest that such data were collected for a wider range of dates). These are organized by boroughs and city-wide totals are available for our purposes. See Figure S6 for a sample table providing city-wide totals, and §S3 for a sample of a full weekly report.

S1.3 NYC Health Dept. Vital Statistics Reports: 1900–1984

The NYC Health Dept. website has made historical vital statistics reports available to the general public [2]. These reports, for the years of 1976–1984, contain tables showing city-wide monthly aggregated cases of reportable diseases. For years outside of this range and going back to 1935, yearly aggregated data is provided in the reports we obtained. For disease incidence, yearly data is by no means sufficient for our purposes. However, these vital statistics reports, as the name would imply, contain population and vital statistics data, for which yearly numbers are adequate. Furthermore, 5-year estimates are reported from 1900–1935.

S1.4 1915

We noted previously that we must further discuss the Weekly Bulletin data for the year 1915. Disease incidence numbers prior to 1915 come from Volume 1 of the Health Bulletins, and after 1915 come from Volume 2, as noted previously. The data before and after 1915 represent measles cases for all of NYC, whereas the data we have for 1915 represent counts taken for only three hospitals within the city. Using yearly aggregated reported measles cases taken from the NYC Vital Statistics Reports [2] and comparing them with yearly totals from the Health Bulletin data (see Figure S10), we determine a scaling factor (5.04) with which to adjust the weekly Health Bulletin Data. Figure S7 shows measles incidence rates recorded for the years surrounding 1915 before we re-sale the 1915 data. We conclude from the apparent consistency in the pattern of outbreaks that the adjustment is appropriate.

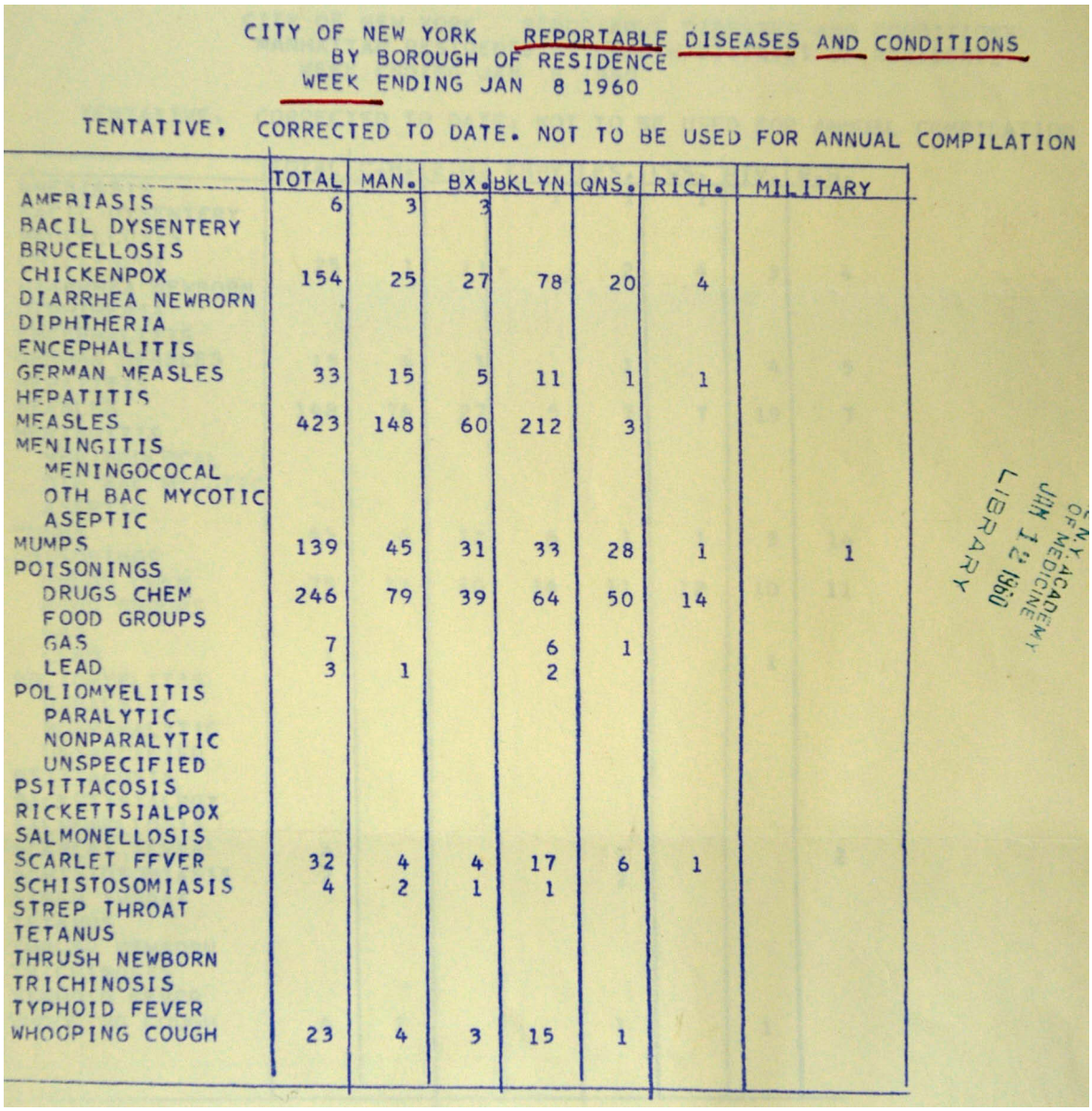

CITY OF NEW YORK REPORTABLE DISEASES AND CONDITIONS
BY BOROUGH OF RESIDENCE
WEEK ENDING JAN 8 1960

TENTATIVE, CORRECTED TO DATE. NOT TO BE USED FOR ANNUAL COMPILATION

	TOTAL	MAN.	BX.	BKLYN	QNS.	RICH.	MILITARY
AMEBIASIS	6	3	3				
BACIL DYSENTERY							
BRUCELLOSIS							
CHICKENPOX	154	25	27	78	20	4	
DIARRHEA NEWBORN							
DIPHTHERIA							
ENCEPHALITIS							
GERMAN MEASLES	33	15	5	11	1	1	
HEPATITIS							
MEASLES	423	148	60	212	3		
MENINGITIS							
MENINGOCOCAL							
OTH BAC MYCOTIC							
ASEPTIC							
MUMPS	139	45	31	33	28	1	1
POISONINGS							
DRUGS CHEM	246	79	39	64	50	14	
FOOD GROUPS							
GAS	7			6	1		
LEAD	3	1		2			
POLIOMYELITIS							
PARALYTIC							
NONPARALYTIC							
UNSPECIFIED							
PSITTACOSIS							
RICKETTSIALPOX							
SALMONELLOSIS							
SCARLET FEVER	32	4	4	17	6	1	
SCHISTOSOMIASIS	4	2	1	1			
STREP THROAT							
TETANUS							
THRUSH NEWBORN							
TRICHINOSIS							
TYPHOID FEVER							
WHOOPING COUGH	23	4	3	15	1		

Figure S6: NYC Health Dept. table showing reportable diseases and conditions. See §S3 for full weekly report.

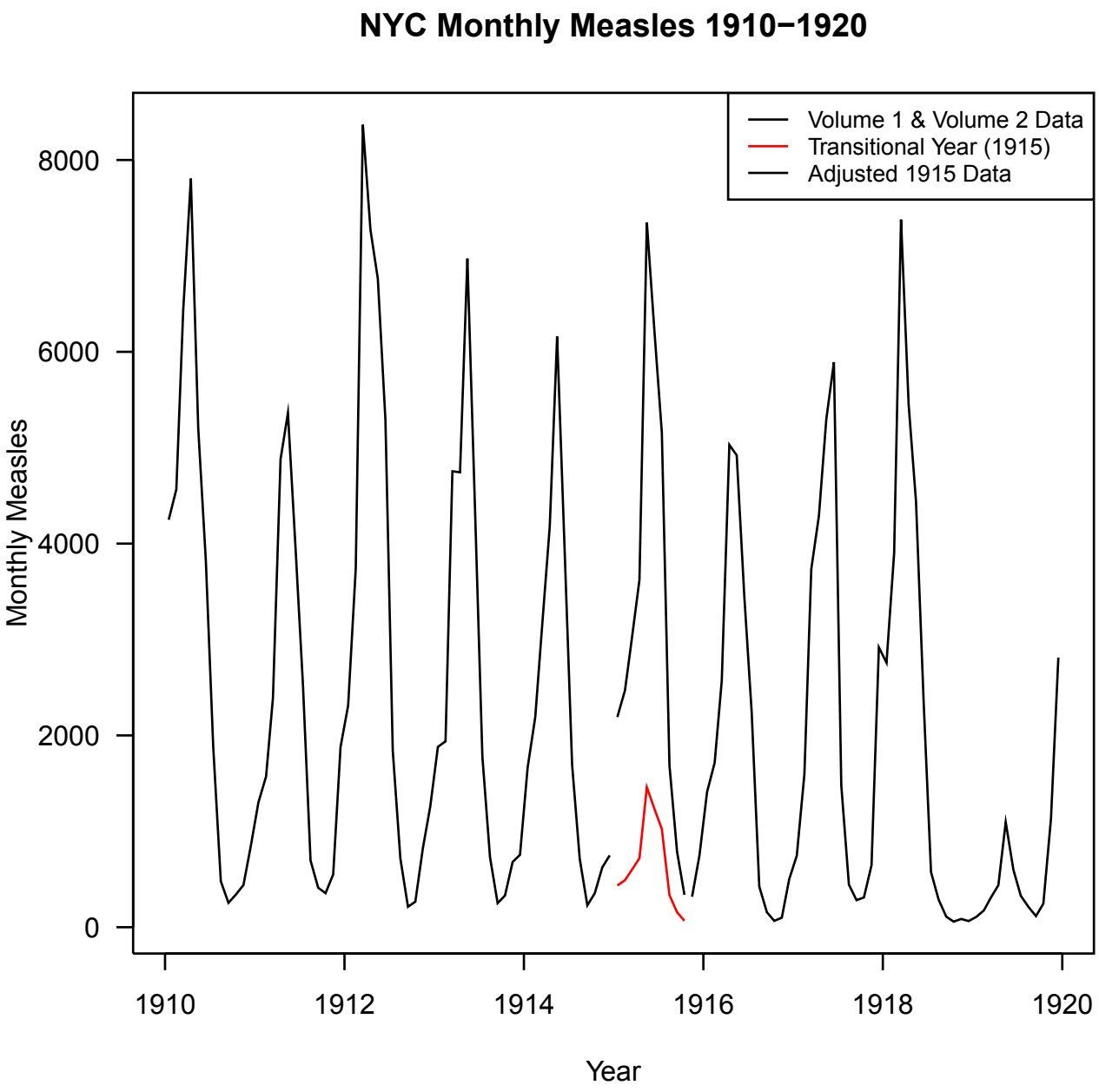

Figure S7: Time series plot of tabulated Health Bulletin data from 1910–1920, showing original and adjusted 1915 reported measles cases from three hospitals in the context of city-wide measles cases for other years.

S1.5 Formatting the Data

For our analysis, we make use of weekly and monthly aggregated measles data, and yearly vital data. For large time spans (namely 1932–1958 and 1976–1984), we have only monthly data, hence we interpolate pseudo-weekly data from the monthly data points.

For vital statistics, we obtain yearly total population and birth rates from the NYC Health Bulletins for 1891–1900 as detailed previously §S1.1.2, and from the NYC Dept. of Health vital statistics reports for 1900–1984. Note that the vital statistics reports contain only data points every 5 years from 1900–1935.

We do not interpolate yearly points from this because the Vital Statistics Reports give a single estimate for each of the 5-years.

S1.6 Summary of Available and Compiled Data

Since we are using data from various overlapping sources, we need to pick time points where we transition from one source to the next. Since it is better to do analyses using originally recorded weekly data rather than pseudo-weekly interpolation, we will use as much originally recorded weekly data as possible.

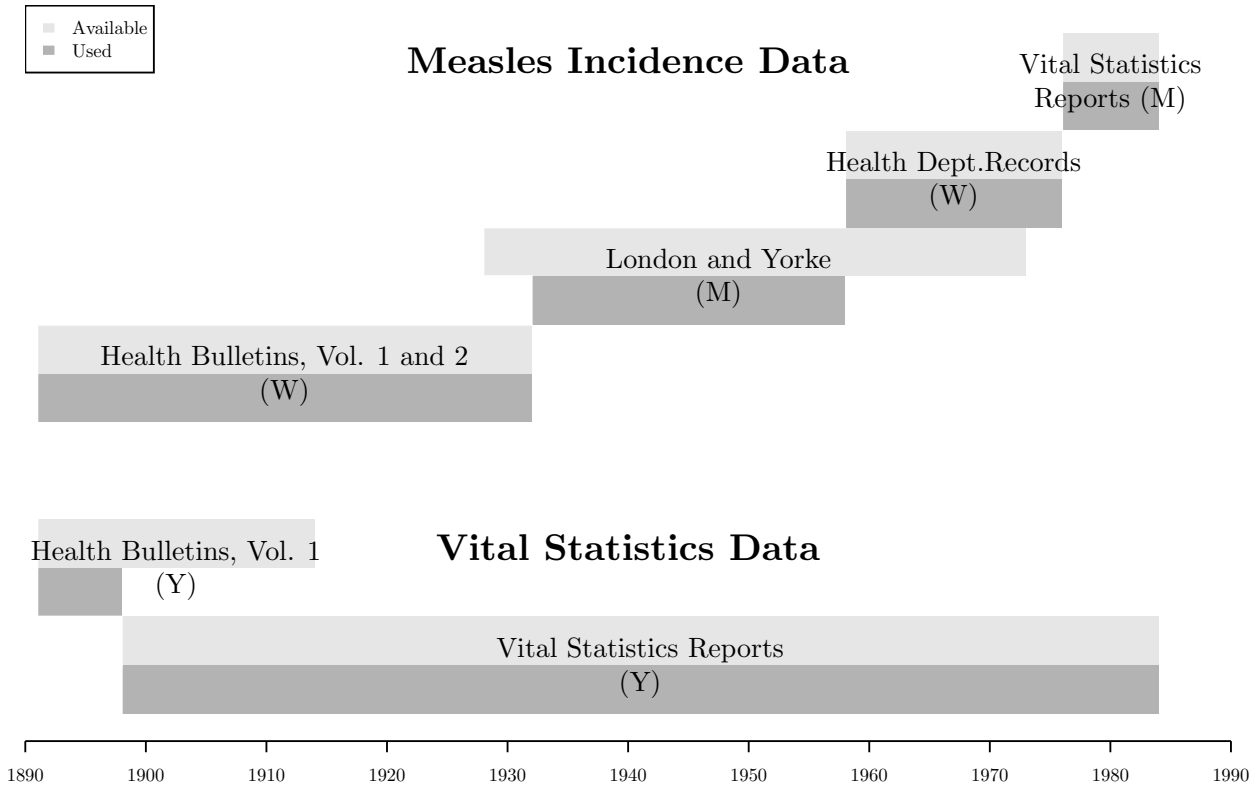

Figure S8: Summary of available and used data.

S1.7 Normalized Data

For our analysis of the disease incidence data, we need to control for changes in population size. To this end we have constructed a time series of yearly total population numbers, as detailed previously. Using the population data, we can normalize disease incidence data with respect to population size. This serves to remove elements of the dynamics which are simply artifacts of changes in population, and what remains is a more consistent representation of the dynamics of measles. See Figure S9 for a plot of total population with respect to time, which we use to normalize our data. Note in particular the high rate of population growth in the early 1900s; much of an apparent rise in measles incidence can be attributed to this. The sudden jump in the population data is attributed to a change in reporting area (see §S1.1)

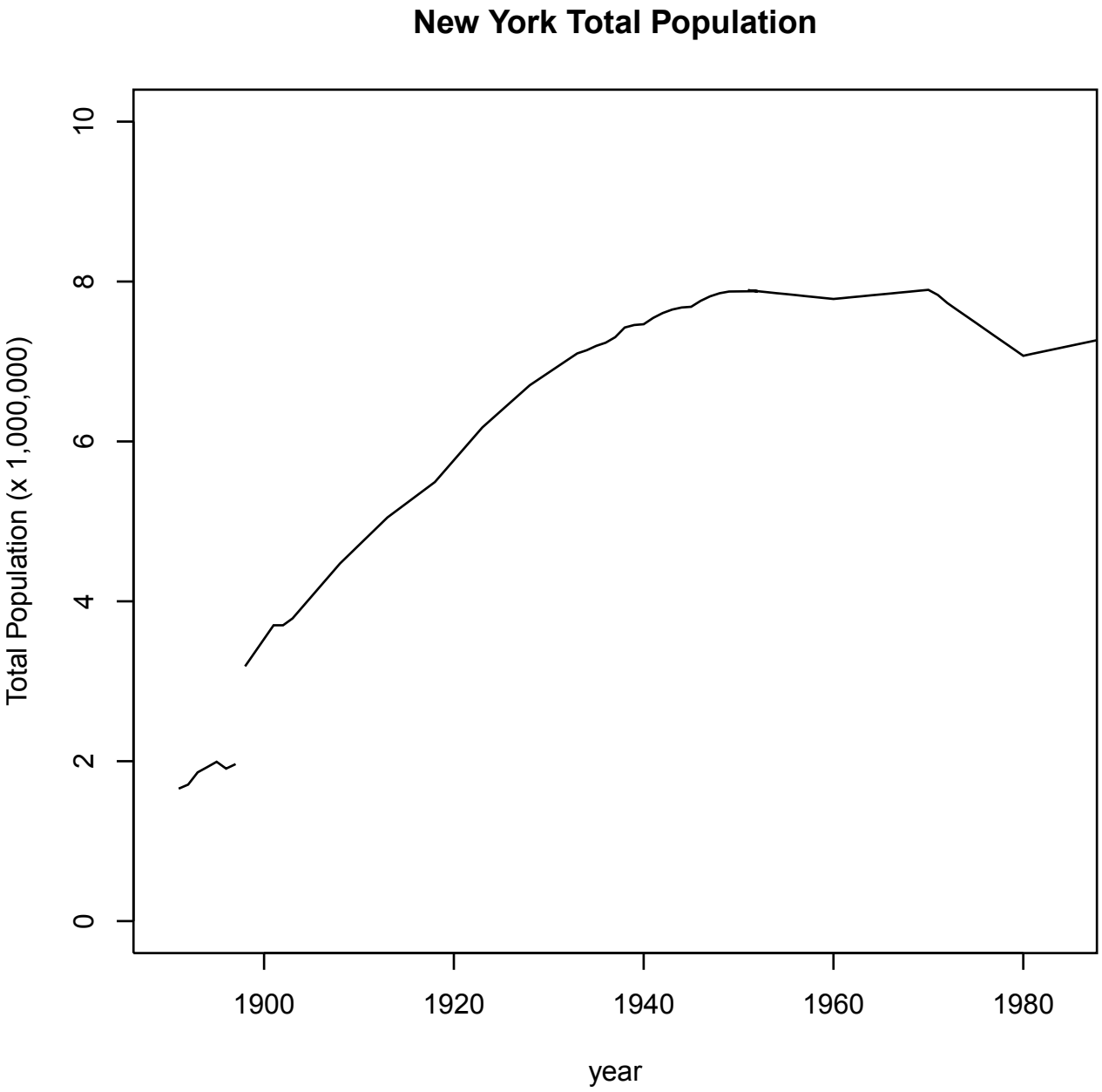

Figure S9: Time series plot of the total population of NYC from 1891–1984.

S1.8 Consistency Checks

Since much of the data we use is from original digitization, it is appropriate to conduct a number of checks on the data to ensure that its quality is acceptable for the analysis. We therefore cross-reference our new data with as much independent information as we can. To this end we perform the following three sanity checks on our new data:

1. The NYC Health Department Vital Statistics Reports [2] list yearly totals for disease incidence from 1911 to the present. Our first check takes yearly sums of our weekly data from the Health Bulletins

in the time-span of 1911–1932, and compares these yearly sums to data from the Health Department Vital Statistics Reports. See Figure S10 for this comparison. We conclude that, with the exception of the year 1915 (which we dealt with previously), the close match of these totals evidences reliability of the Health Bulletin data.

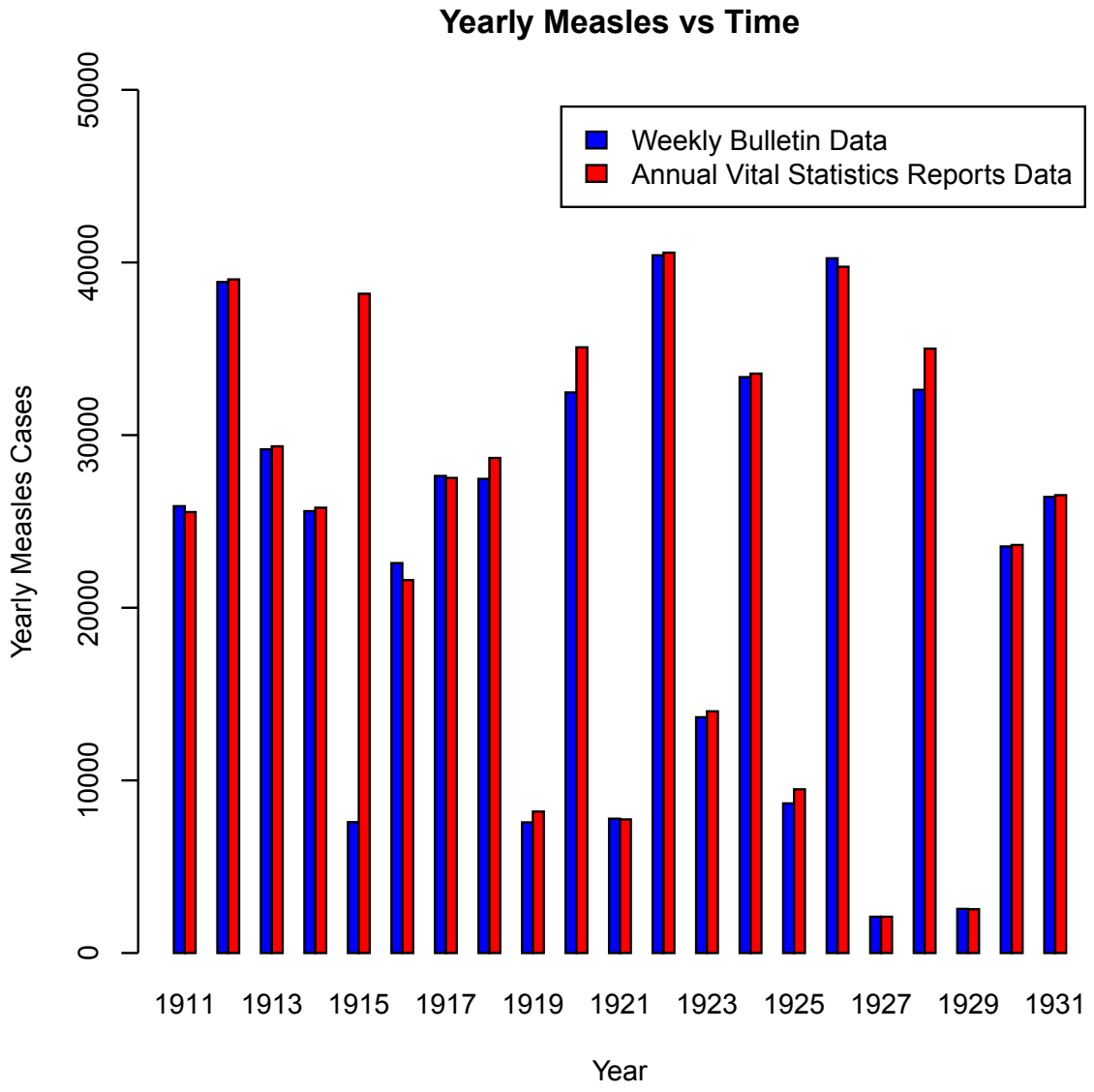

Figure S10: Overlapping time series plots of yearly measles incidence counts taken from the Health Bulletins and the Health Dept. Vital Statistics Reports.

2. Much of the newly digitized data overlaps with monthly data previously published by London and Yorke [11]. We can therefore use monthly tabulated totals of our original weekly data in the overlapping periods and compare them to London and Yorke's data. The results of this second check are shown in Figures S11 and S12. Interestingly, these numbers do not match up perfectly, suggesting that adjustments were made by the NYC Health Department to the data we acquired (both from the Health Bulletins and the Health Department Records), prior to its tabulation in the paper published

in 1973 by London and Yorke [11].[2] The monthly sums of measles cases, however, match up closely enough in both overlapping time periods that we conclude our weekly data are reliable.

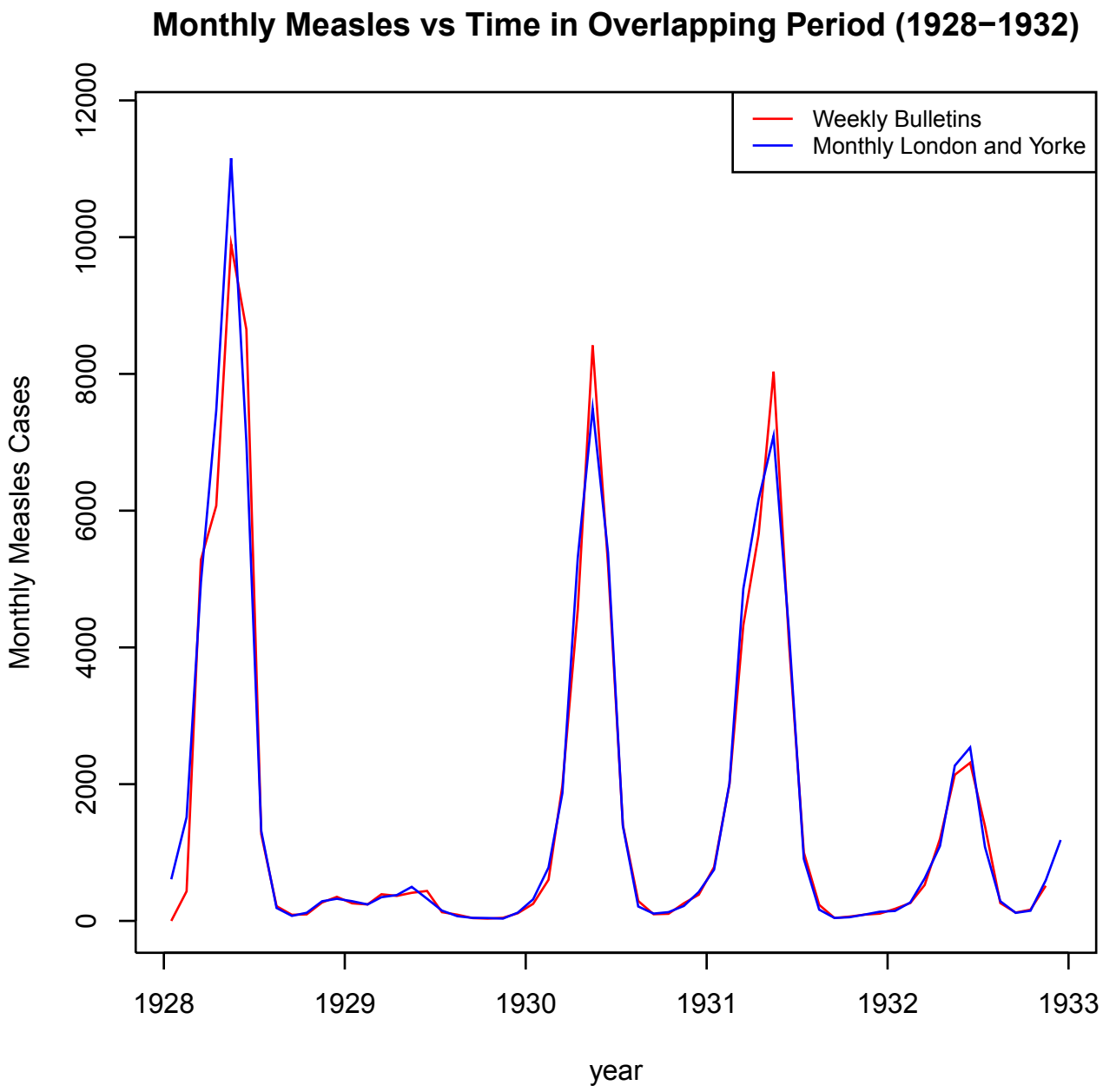

Figure S11: Overlapping time series plots of London and Yorke's monthly measles incidence rates, and the Health Dept. Bulletins weekly measles incidence rates, from 1928–1932. To compare these numbers, we have summed the weekly Bulletin data monthly, summing up the number of measles cases reported at the ends of weeks that fall in the same month.

[2]London and Yorke give very little information regarding the source of the data published their 1973 paper [11], only mentioning that the provider was the NYC Health Dept. Bureau of Infectious Disease Control (which no longer exists).

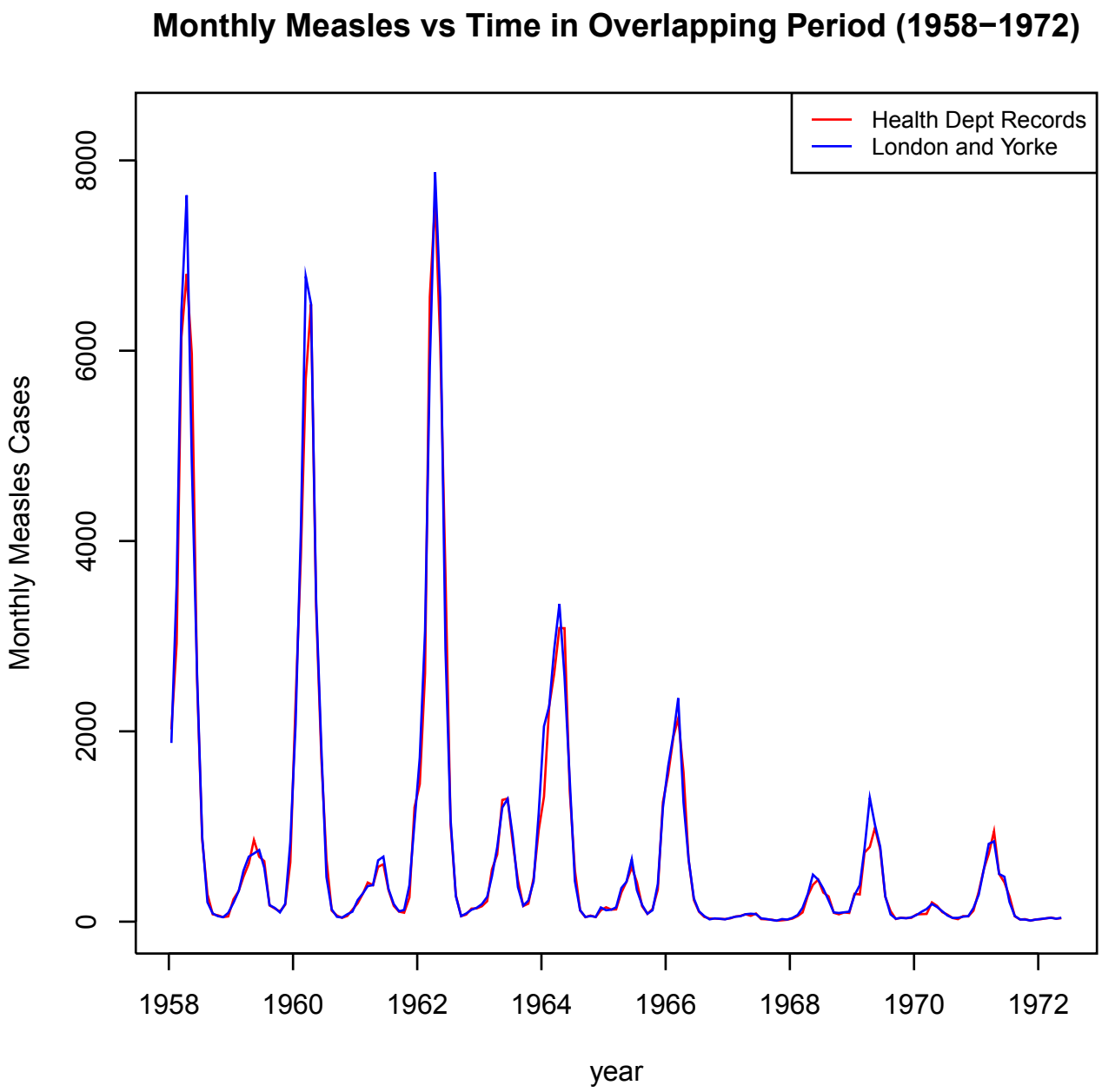

Figure S12: Overlapping time series plots of London and Yorke's monthly measles incidence rates, and the Health Dept. Records weekly incidence rates summed monthly, from 1958–1973.

Jan 31, 1920 In Figure S13, we show a page from the Weekly Bulletins in which an epidemic of influenza can be seen from the case reports, peaking on Jan 31, 1920 with a number of reported cases of 30456. For this same week, the cases of measles are reported as 4671, where the previous and following weeks were 1984 and 2035, respectively. Such a high number of reported measles cases seems unlikely, and possibly erroneously entered, but could otherwise have been misdiagnoses from the influenza outbreak.

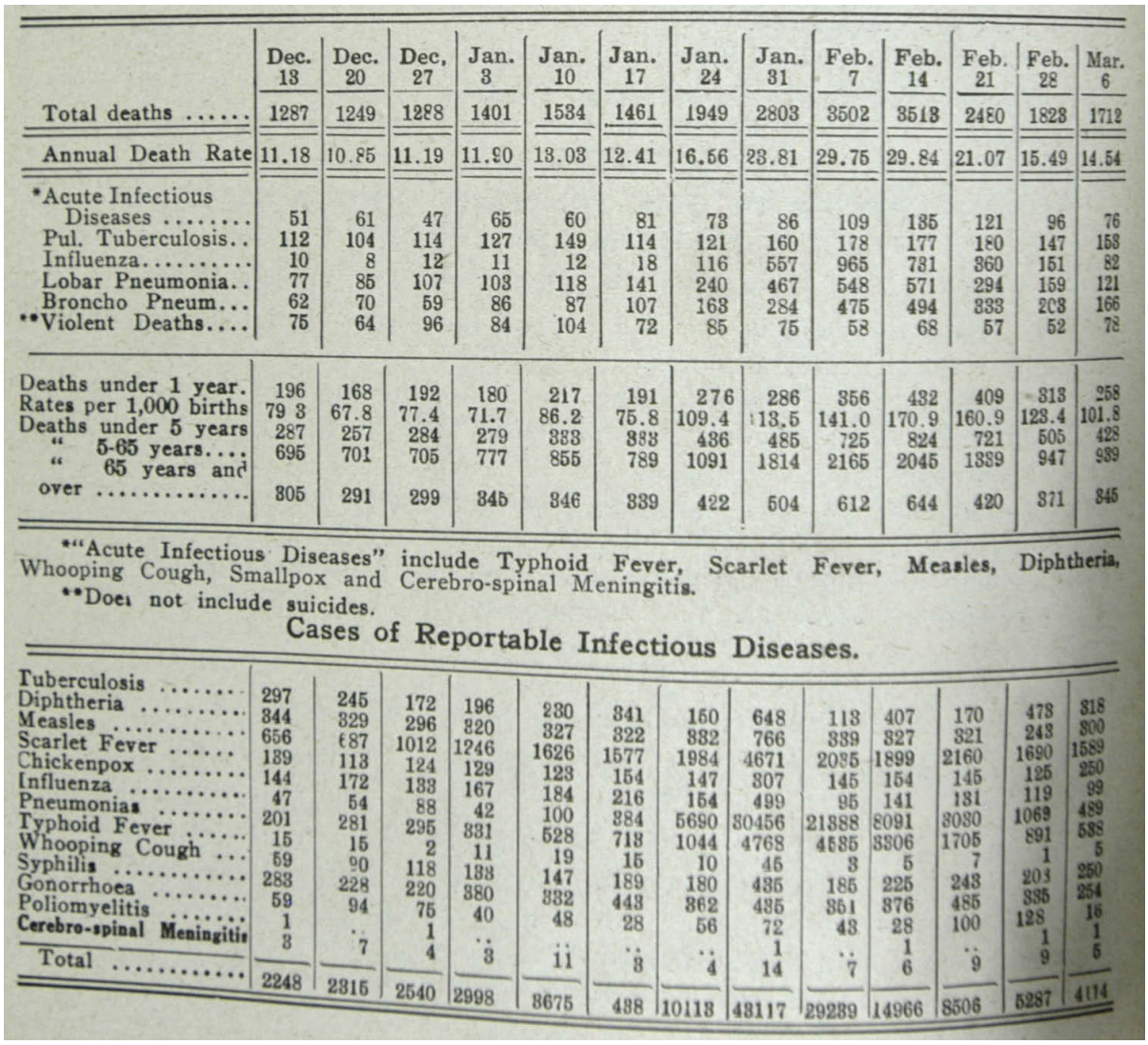

	Dec. 13	Dec. 20	Dec. 27	Jan. 3	Jan. 10	Jan. 17	Jan. 24	Jan. 31	Feb. 7	Feb. 14	Feb. 21	Feb. 28	Mar. 6
Total deaths	1287	1249	1288	1401	1534	1461	1949	2803	3502	3513	2480	1828	1712
Annual Death Rate	11.18	10.85	11.19	11.90	13.03	12.41	16.56	23.81	29.75	29.84	21.07	15.49	14.54
*Acute Infectious Diseases	51	61	47	65	60	81	73	86	109	135	121	96	76
Pul. Tuberculosis..	112	104	114	127	149	114	121	160	178	177	180	147	153
Influenza.....	10	8	12	11	12	18	116	557	965	781	360	151	82
Lobar Pneumonia..	77	85	107	103	118	141	240	467	548	571	294	159	121
Broncho Pneum...	62	70	59	86	87	107	163	284	475	494	333	203	166
**Violent Deaths....	75	64	96	84	104	72	85	75	58	68	57	52	78
Deaths under 1 year.	196	168	192	180	217	191	276	286	356	432	409	313	258
Rates per 1,000 births	79 3	67.8	77.4	71.7	86.2	75.8	109.4	113.5	141.0	170.9	160.9	123.4	101.8
Deaths under 5 years	287	257	284	279	333	333	436	485	725	824	721	505	428
" 5-65 years....	695	701	705	777	855	789	1091	1814	2165	2045	1339	947	939
" 65 years and over	305	291	299	345	346	339	422	504	612	644	420	371	345

*"Acute Infectious Diseases" include Typhoid Fever, Scarlet Fever, Measles, Diphtheria, Whooping Cough, Smallpox and Cerebro-spinal Meningitis.

**Does not include suicides.

Cases of Reportable Infectious Diseases.

Tuberculosis	297	245	172	196	230	341	150	648	113	407	170	473	318
Diphtheria	344	329	296	320	327	322	332	766	339	327	321	243	300
Measles	656	687	1012	1246	1626	1577	1984	4671	2085	1899	2160	1690	1589
Scarlet Fever	139	113	124	129	123	154	147	307	145	154	145	125	250
Chickenpox	144	172	133	167	184	216	154	499	95	141	131	119	99
Influenza	47	54	88	42	100	384	5690	30456	21388	8091	3030	1069	489
Pneumonias	201	281	295	331	528	718	1044	4768	4585	3306	1705	891	538
Typhoid Fever	15	15	2	11	19	15	10	45	3	5	7	1	5
Whooping Cough ...	59	90	118	133	147	189	180	435	185	225	243	203	250
Syphilis	283	228	220	380	332	443	362	435	351	376	485	335	254
Gonorrhoea	59	94	75	40	48	28	56	72	43	28	100	128	16
Poliomyelitis	1	..	1	..	..	..	..	1	..	1	..	1	1
Cerebro-spinal Meningitis	3	7	4	3	11	3	4	14	7	6	9	9	5
Total	2248	2315	2540	2998	3675	438	10113	43117	29289	14966	8506	5287	4114

Figure S13: Weekly Bulletins pages showing weekly reported cases for infectious diseases from 13 December 1919 to 6 March 1920. The reported number of cases of measles for the week of 31 January is unusually high (no other weekly count exceeds 2500 until the year 1941). Concurrent with an apparent measles epidemic is an influenza epidemic, which suggests that the 31 January reported number—and possibly others— could result from misdiagnoses. It is also possible that the unusually high number, if it is incorrect, resulted from a clerical error.

S2 Transient Periods in Wavelet Spectra

A wavelet spectrum of an epidemic time series typically has peaks at the periodicities of attractors that the system visits. However, transient periods do not reveal themselves as consistently as attractor periods, since they depend on demographic stochasticity to be maintained [3,4,7]. The distance of the system from a periodic attractor is influenced by random stochastic perturbations, and the spectral power of transient periods in the time series depends on this distance. As a result, we should expect significant lack of homogeneity in the spectral power of transient periods in disease time series.

To verify this intuition, we simulated many realizations of the stochatic SIR model, and we show wavelet spectra [5, 6, 9, 10, 12] of a subset of these simulated time series in Figures S14 to S19. In order to produce simulated time series comparable to our NYC measles time series, we produced simulations of the same length as the measles time series. We produced 10 stochastic SIR realizations for each of 6 different parameter sets. Three parameter sets fixed $\mu = \nu = 0.02/\text{year}$, and the other three parameter sets were defined using birth and death rates derived from NYC vital statistics. In both groups of parameter sets, we considered three $\mathcal{R}_0$ values ($\mathcal{R}_0 \in \{12, 14.5, 17\}$). The mean infectious period was set to 13 days in all simulations, and the initial total population was fixed at the NYC population in 1891 (the beginning of the time series). For each parameter set, we show one of the 10 realizations in Figures S14 to S19.

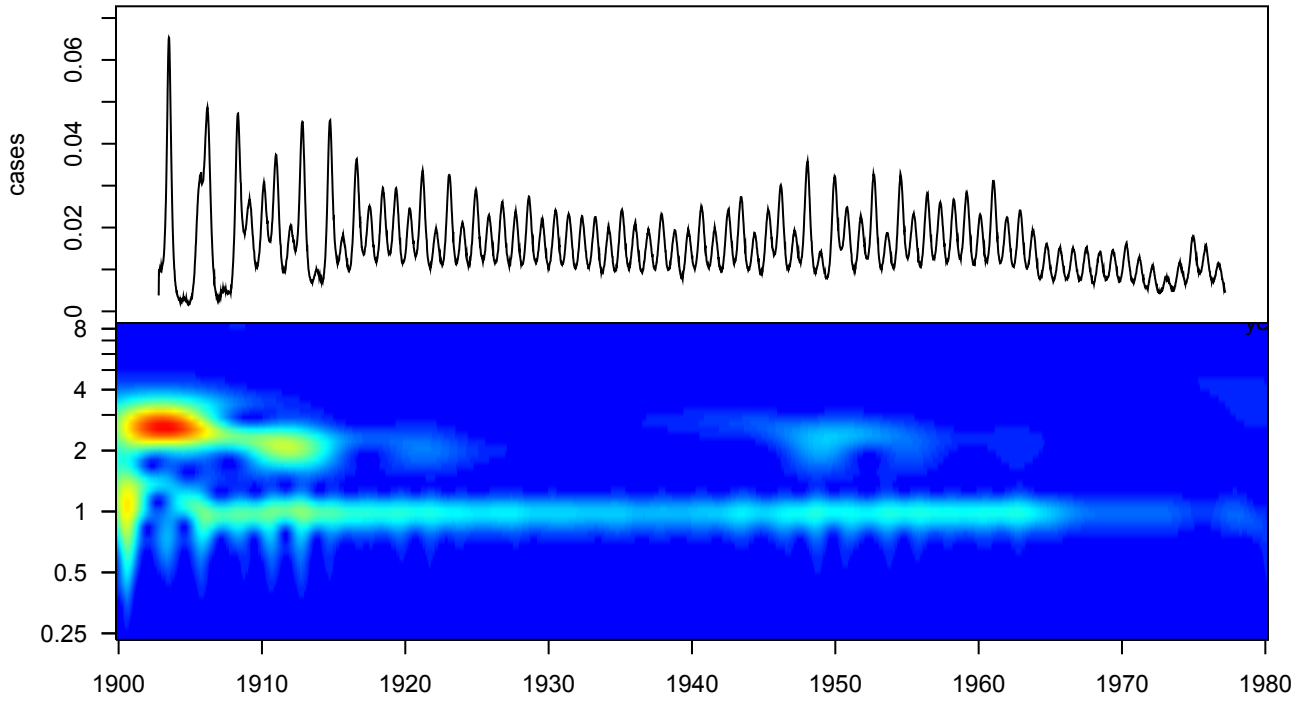

Figure S14: Stochastic SIR simulation emulating NYC. *Top panel:* cases time series. *Bottom panel:* wavelet spectrum. *Parameter values:* $\mathcal{R}_0 = 12$, $1/\gamma = 13$ days, $\mu = \nu = 0.02\,\mathrm{yr}^{-1}$.

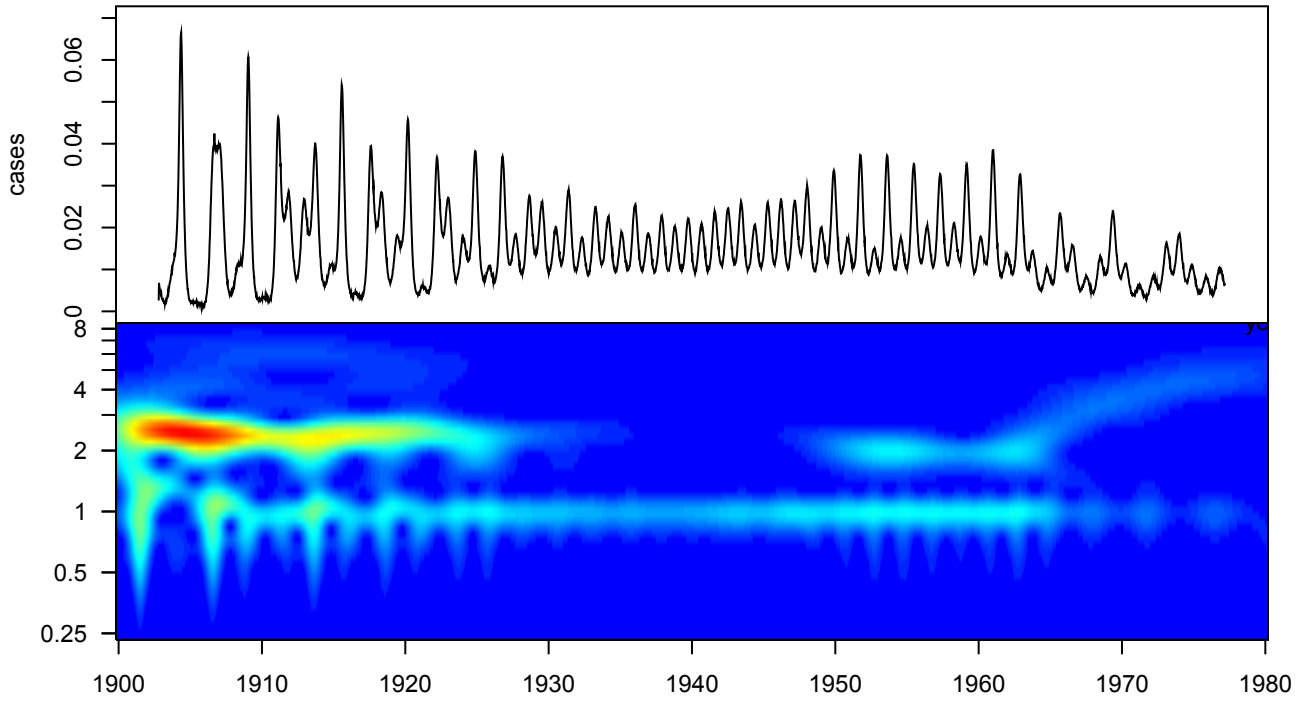

Figure S15: Stochastic SIR simulation emulating NYC. *Top panel:* cases time series. *Bottom panel:* wavelet spectrum. *Parameter values:* $\mathcal{R}_0 = 14.5$, $1/\gamma = 13$ days, $\mu = \nu = 0.02\,\mathrm{yr}^{-1}$.

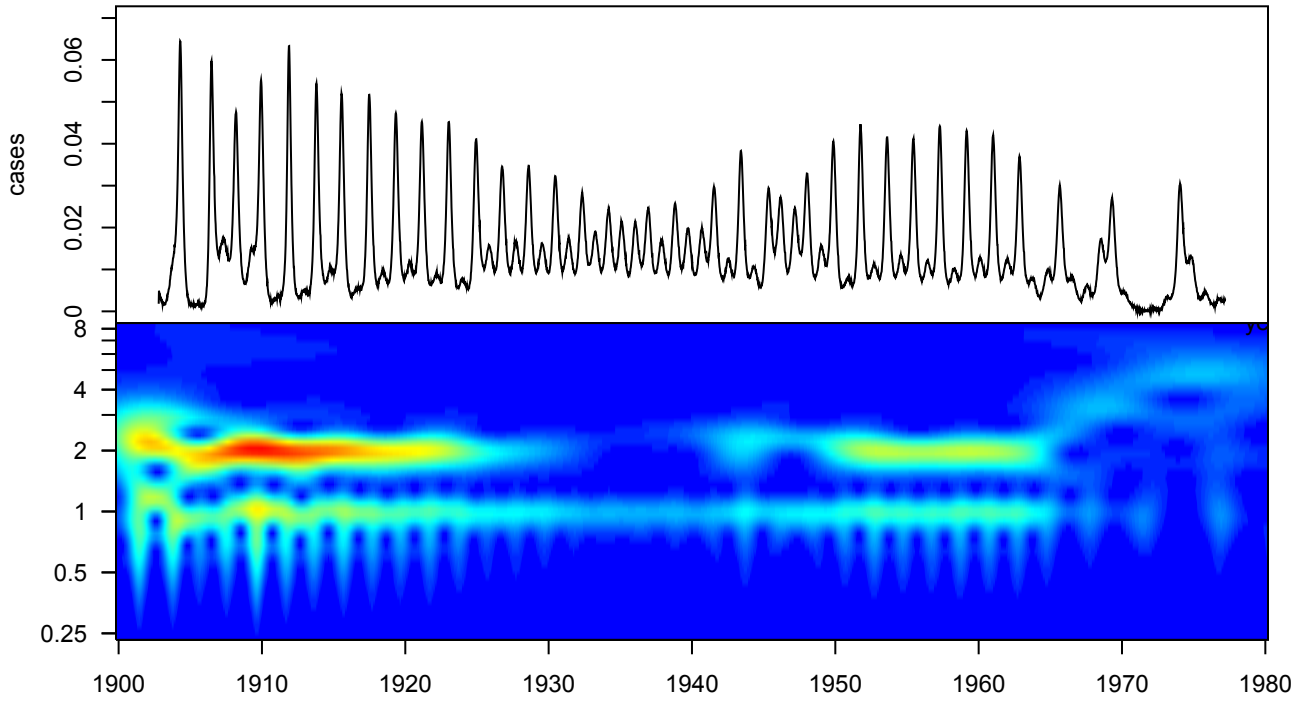

Figure S16: Stochastic SIR simulation emulating NYC. *Top panel:* cases time series. *Bottom panel:* wavelet spectrum. *Parameter values:* $\mathcal{R}_0 = 17$, $1/\gamma = 13$ days, $\mu = \nu = 0.02\,\mathrm{yr}^{-1}$.

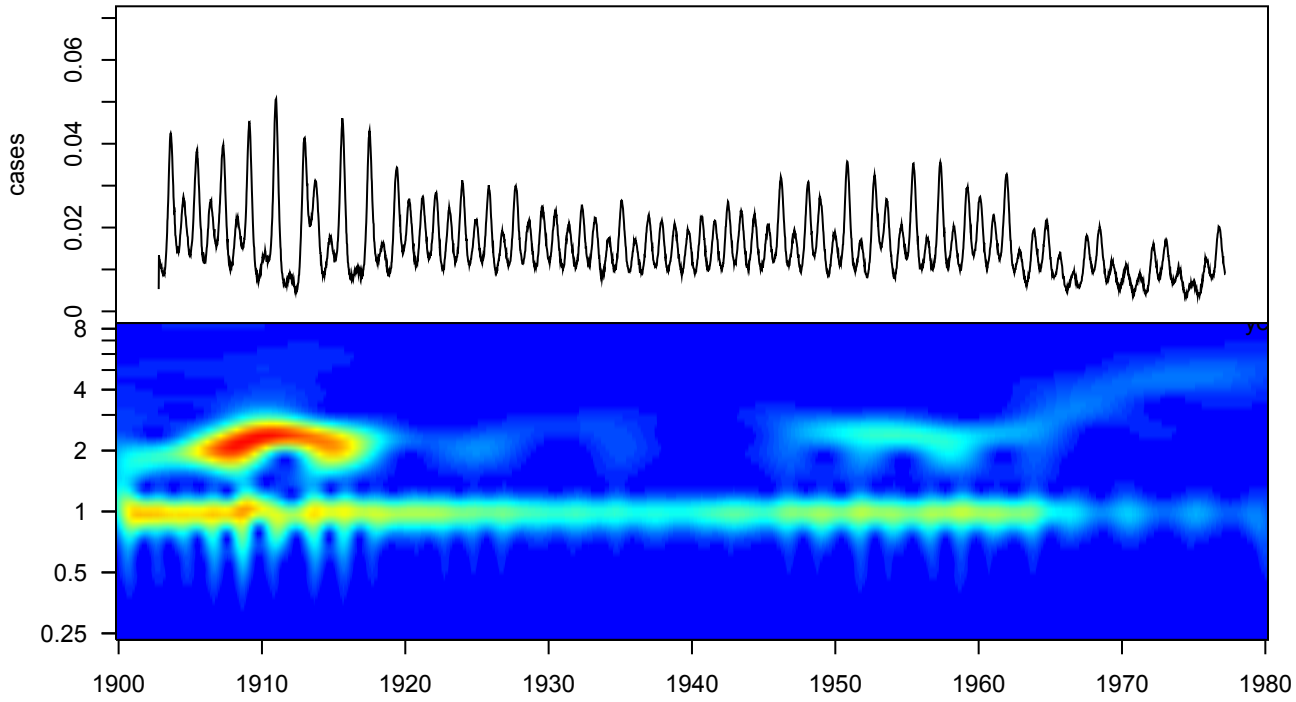

Figure S17: Stochastic SIR simulation emulating NYC. *Top panel:* cases time series. *Bottom panel:* wavelet spectrum. *Parameter values:* $\mathcal{R}_0 = 12$, $1/\gamma = 13$ days, $\mu(t)$ and $\nu(t)$ are realistic NYC values changing with time.

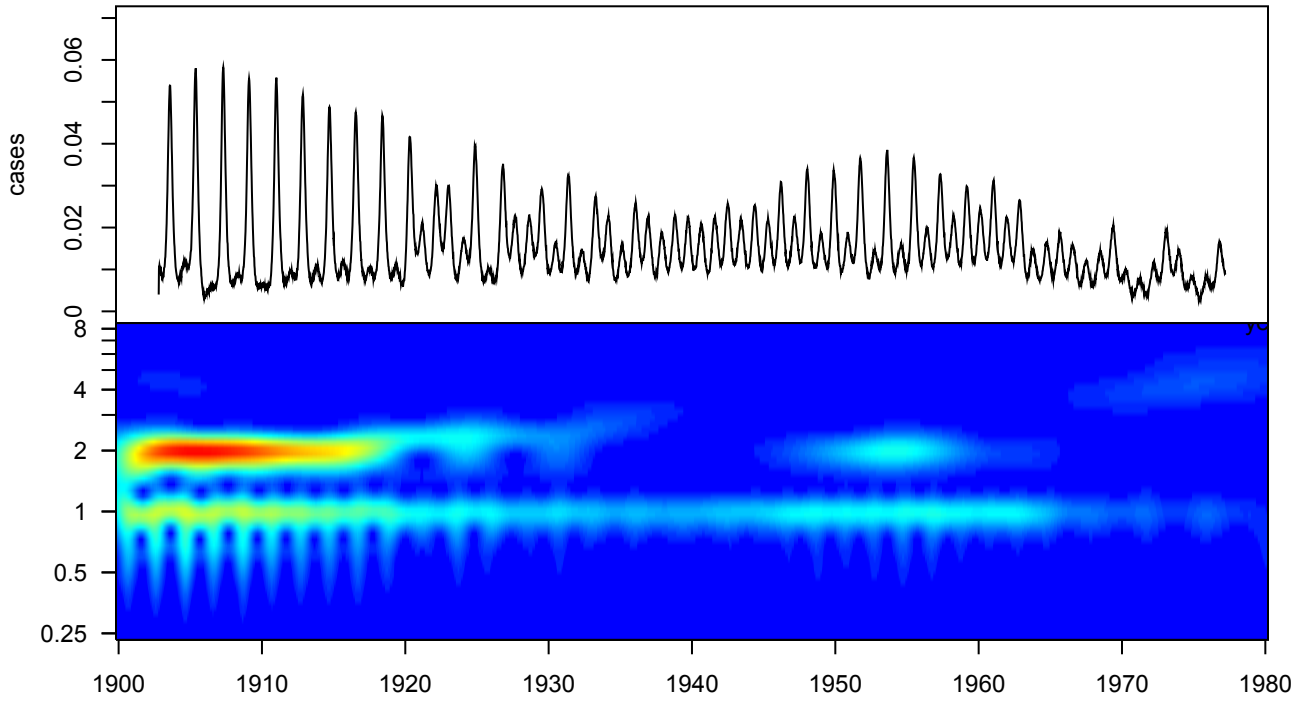

Figure S18: Stochastic SIR simulation emulating NYC. *Top panel:* cases time series. *Bottom panel:* wavelet spectrum. *Parameter values:* $\mathcal{R}_0 = 14.5$, $1/\gamma = 13$ days, $\mu(t)$ and $\nu(t)$ are realistic NYC values changing with time.

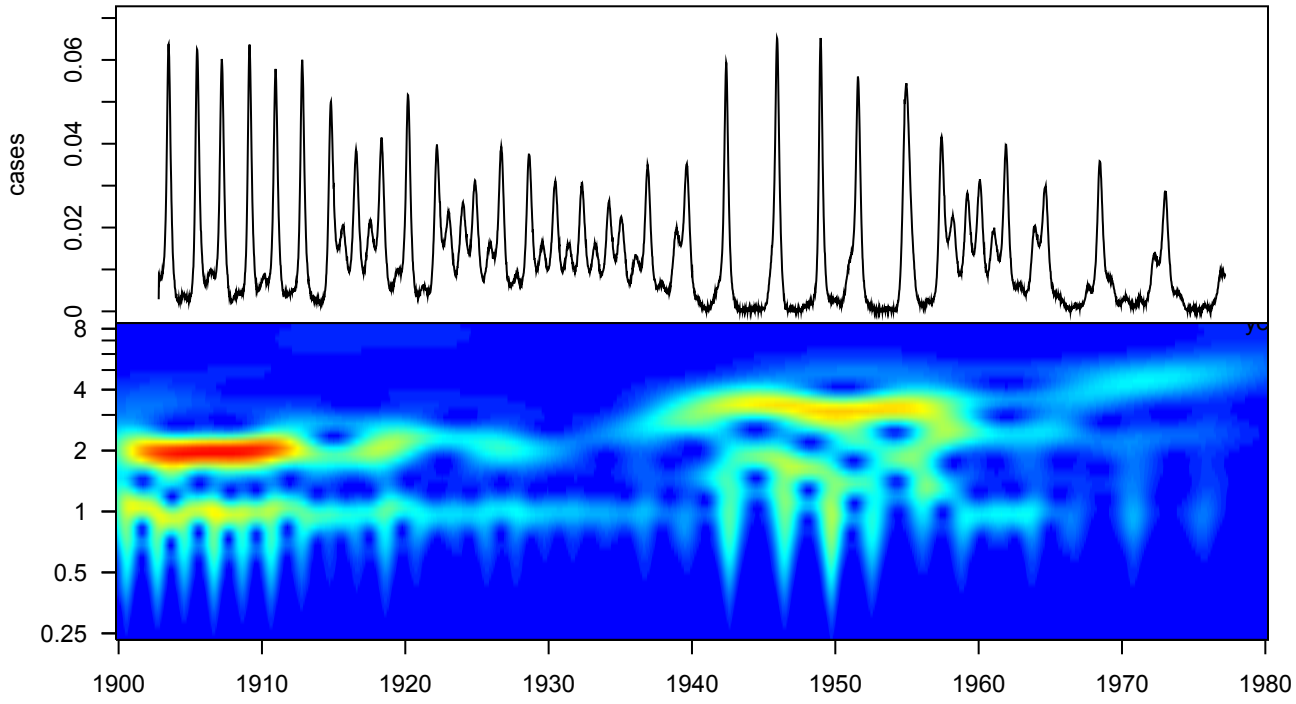

Figure S19: Stochastic SIR simulation emulating NYC. *Top panel:* cases time series. *Bottom panel:* wavelet spectrum. *Parameter values:* $\mathcal{R}_0 = 17$, $1/\gamma = 13$ days, $\mu(t)$ and $\nu(t)$ are realistic NYC values changing with time.

S3 Sample Photographs from Data Sources

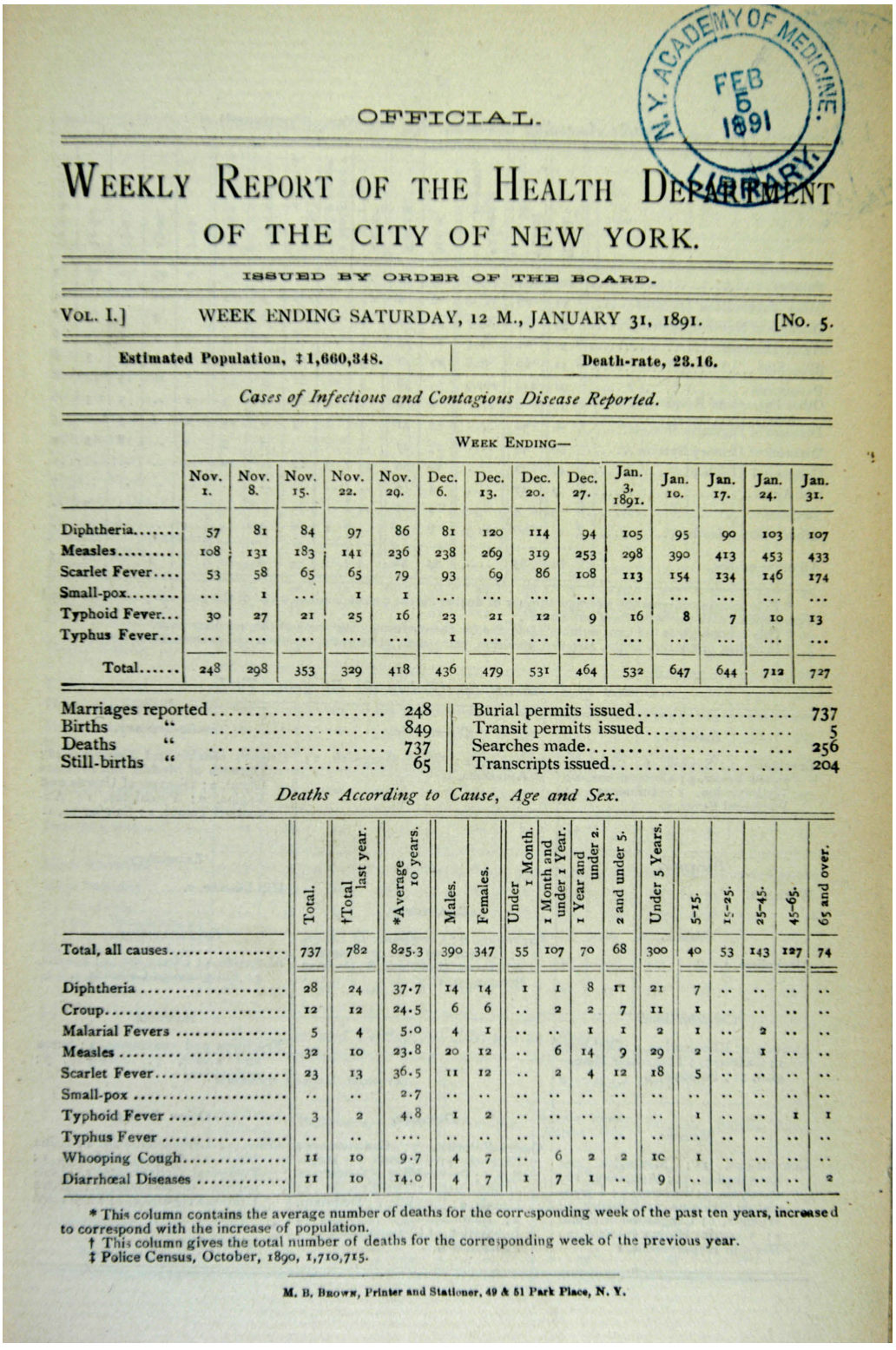

OFFICIAL.

WEEKLY REPORT OF THE HEALTH DEPARTMENT OF THE CITY OF NEW YORK.

ISSUED BY ORDER OF THE BOARD.

VOL. I.] WEEK ENDING SATURDAY, 12 M., JANUARY 31, 1891. [No. 5.

Estimated Population, ‡1,660,348. | **Death-rate, 23.16.**

Cases of Infectious and Contagious Disease Reported.

	Week Ending—													
	Nov. 1.	Nov. 8.	Nov. 15.	Nov. 22.	Nov. 29.	Dec. 6.	Dec. 13.	Dec. 20.	Dec. 27.	Jan. 3, 1891.	Jan. 10.	Jan. 17.	Jan. 24.	Jan. 31.
Diphtheria	57	81	84	97	86	81	120	114	94	105	95	90	103	107
Measles	108	131	183	141	236	238	269	319	253	298	390	413	453	433
Scarlet Fever	53	58	65	65	79	93	69	86	108	113	154	134	146	174
Small-pox	...	1	...	1	1	...	...	...	...	...	...	...	...	...
Typhoid Fever	30	27	21	25	16	23	21	12	9	16	8	7	10	13
Typhus Fever	...	...	...	...	...	1	...	...	...	...	...	...	...	...
Total	248	298	353	329	418	436	479	531	464	532	647	644	712	727

Marriages reported	248	Burial permits issued	737
Births "	849	Transit permits issued	5
Deaths "	737	Searches made	256
Still-births "	65	Transcripts issued	204

Deaths According to Cause, Age and Sex.

	Total.	†Total last year.	*Average 10 years.	Males.	Females.	Under 1 Month.	1 Month and under 1 Year.	1 Year and under 2.	2 and under 5.	Under 5 Years.	5–15.	15–25.	25–45.	45–65.	65 and over.
Total, all causes	737	782	825.3	390	347	55	107	70	68	300	40	53	143	127	74
Diphtheria	28	24	37.7	14	14	1	1	8	11	21	7	..	..	..	..
Croup	12	12	24.5	6	6	..	2	2	7	11	1	..	..	..	..
Malarial Fevers	5	4	5.0	4	1	..	..	1	1	2	1	..	2	..	..
Measles	32	10	23.8	20	12	..	6	14	9	29	2	..	1	..	..
Scarlet Fever	23	13	36.5	11	12	..	2	4	12	18	5	..	..	..	..
Small-pox	..	..	2.7	..	..	..	..	..	..	..	..	..	..	..	..
Typhoid Fever	3	2	4.8	1	2	..	..	..	..	..	1	..	..	1	1
Typhus Fever	..	..	....	..	..	..	..	..	..	..	..	..	..	..	..
Whooping Cough	11	10	9.7	4	7	..	6	2	2	10	1	..	..	..	..
Diarrhœal Diseases	11	10	14.0	4	7	1	7	1	..	9	..	..	..	..	2

* This column contains the average number of deaths for the corresponding week of the past ten years, increased to correspond with the increase of population.
† This column gives the total number of deaths for the corresponding week of the previous year.
‡ Police Census, October, 1890, 1,710,715.

M. B. Brown, Printer and Stationer, 49 & 51 Park Place, N. Y.

Figure S20: Weekly Bulletins Vol 1: Page 1

Deaths According to Cause, Annual Rate per 1,000 and Age, with Meteorology, and Number of Deaths in Public Institutions for 13 weeks.

Week Ending	Nov. 8.	Nov. 15.	Nov. 22.	Nov. 29.	Dec. 6.	Dec. 13.	Dec. 20.	Dec. 27.	Jan. 3, 1891.	Jan. 10.	Jan. 17.	Jan. 24.	Jan. 31.
Total deaths	671	643	583	654	672	704	731	705	764	744	786	748	737
Annual death-rate	21.23	20.33	18.43	20.66	21.21	22.21	23.05	22.22	24.06	23.42	24.73	23.52	23.16
Diphtheria	19	27	29	22	31	31	37	31	28	14	19	22	28
Croup	5	17	6	20	14	11	11	14	11	16	22	11	12
Malarial Fevers	5	3	3	1	1	5	3	6	4	2	3	4	5
Measles	13	11	12	12	12	15	15	19	22	15	18	33	32
Scarlet Fever	11	7	10	10	5	10	11	11	21	16	22	20	23
Small-pox	..	..	..	..	..	..	..	..	..	..	..	..	..
Typhoid Fever	10	10	7	5	8	11	3	5	7	3	3	3	3
Typhus Fever	..	..	..	..	..	..	..	..	..	..	..	..	..
Whooping Cough	10	7	7	3	5	7	5	8	9	8	12	17	11
Diarrhœal Diseases	20	11	8	8	10	9	11	9	10	10	9	13	11
Diarrhœal Diseases under 5 years	17	8	3	7	6	6	7	7	6	7	4	8	9
Phthisis	110	85	78	98	94	102	98	96	105	110	98	111	105
Bronchitis	30	40	32	25	35	29	38	22	49	27	38	44	41
Pneumonia	90	72	85	87	95	115	117	126	134	123	136	105	91
Other Diseases of Respiratory Organs	15	23	18	15	24	21	29	18	29	21	28	25	16
Violent Deaths	30	36	25	36	21	28	33	20	31	37	27	21	18
Under one year	140	134	109	133	120	126	142	130	152	140	165	157	162
Under five years	226	225	204	225	212	240	260	247	290	253	285	284	300
Five to sixty-five	369	352	320	355	371	375	393	374	390	406	403	384	363
Sixty-five years and over	76	66	59	74	89	89	78	84	84	85	98	80	74
In Public Institutions	134	138	128	141	133	133	170	150	140	161	179	136	166
Inquest Cases	73	89	76	85	73	89	87	80	91	110	87	70	83
Mean barometer	29.931	30.103	29.833	29.901	29.850	29.819	29.995	29.904	29.866	30.077	29.823	29.879	29.919
Mean humidity	73	80	68	68	67	60	61	61	57	55	59	65	62
Inches of rain	....	.39	.32	....	1.00	.05	1.87	.77	.80	.07	2.38	1.42	1.46
Mean temperature (Fahrenheit)	48.9	47.2	45.9	35.2	32.0	29.7	32.0	31.5	29.0	25.7	34.6	36.5	38.9
Maximum temperature (Fahrenheit)	69°	60°	64°	59°	49°	47°	43°	47°	54°	41°	51°	53°	48°
Minimum temperature (Fahrenheit)	36°	37°	31°	19°	18°	16°	16°	15°	13°	17°	25°	23°	28°

Infectious and Contagious Diseases in Hospital.

	Willard Parker Hospital.			Riverside Hospital.				
	Scarlet Fever (Children).	Diphtheria.	Total.	Small-pox.	Scarlet Fever. (Adults Only.)	Measles.	Others.	Total.
Remaining Jan. 24	26	3	29	..	19	22	4	45
Admitted	10	6	16	..	4	10	3	17
Discharged	3	4	7	..	3	12	1	16
Died	3	..	3	..	..	2	..	2
Remaining Jan. 31	30	5	35	..	20	18	6	44
Total treated	36	9	45	..	23	32	7	62

Figure S21: Weekly Bulletins Vol 1: Page 2

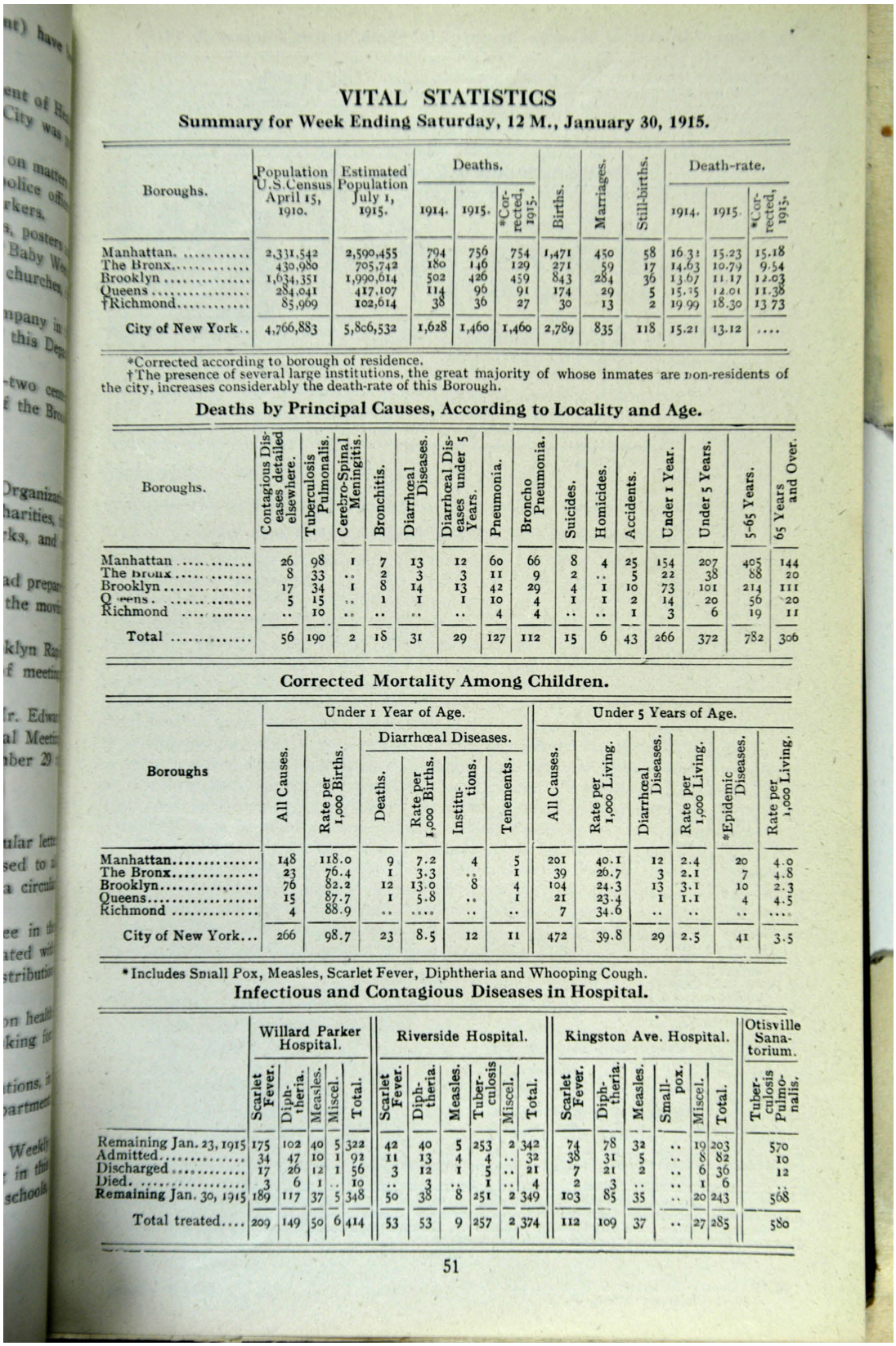

VITAL STATISTICS

Summary for Week Ending Saturday, 12 M., January 30, 1915.

Boroughs.	Population U.S.Census April 15, 1910.	Estimated Population July 1, 1915.	Deaths. 1914.	Deaths. 1915.	Deaths. *Corrected, 1915.	Births.	Marriages.	Still-births.	Death-rate. 1914.	Death-rate. 1915.	Death-rate. *Corrected, 1915.
Manhattan	2,331,542	2,590,455	794	756	754	1,471	450	58	16.31	15.23	15.18
The Bronx	430,980	705,742	180	146	129	271	59	17	14.63	10.79	9.54
Brooklyn	1,634,351	1,990,614	502	426	459	843	284	36	13.67	11.17	12.03
Queens	284,041	417,107	114	96	91	174	29	5	15.75	12.01	11.38
†Richmond	85,969	102,614	38	36	27	30	13	2	19.99	18.30	13.73
City of New York	4,766,883	5,806,532	1,628	1,460	1,460	2,789	835	118	15.21	13.12	....

*Corrected according to borough of residence.

†The presence of several large institutions, the great majority of whose inmates are non-residents of the city, increases considerably the death-rate of this Borough.

Deaths by Principal Causes, According to Locality and Age.

Boroughs.	Contagious Diseases detailed elsewhere.	Tuberculosis Pulmonalis.	Cerebro-Spinal Meningitis.	Bronchitis.	Diarrhœal Diseases.	Diarrhœal Diseases under 5 Years.	Pneumonia.	Broncho Pneumonia.	Suicides.	Homicides.	Accidents.	Under 1 Year.	Under 5 Years.	5-65 Years.	65 Years and Over.
Manhattan	26	98	1	7	13	12	60	66	8	4	25	154	207	405	144
The Bronx	8	33	..	2	3	3	11	9	2	..	5	22	38	88	20
Brooklyn	17	34	1	8	14	13	42	29	4	1	10	73	101	214	111
Queens	5	15	..	1	1	1	10	4	1	1	2	14	20	56	20
Richmond	..	10	..	..	..	..	4	4	..	..	1	3	6	19	11
Total	56	190	2	18	31	29	127	112	15	6	43	266	372	782	306

Corrected Mortality Among Children.

Boroughs	Under 1 Year of Age. All Causes.	Under 1 Year of Age. Rate per 1,000 Births.	Under 1 Year of Age. Diarrhœal Diseases. Deaths.	Under 1 Year of Age. Diarrhœal Diseases. Rate per 1,000 Births.	Under 1 Year of Age. Diarrhœal Diseases. Institutions.	Under 1 Year of Age. Diarrhœal Diseases. Tenements.	Under 5 Years of Age. All Causes.	Under 5 Years of Age. Rate per 1,000 Living.	Under 5 Years of Age. Diarrhœal Diseases.	Under 5 Years of Age. Rate per 1,000 Living.	Under 5 Years of Age. *Epidemic Diseases.	Under 5 Years of Age. Rate per 1,000 Living.
Manhattan	148	118.0	9	7.2	4	5	201	40.1	12	2.4	20	4.0
The Bronx	23	76.4	1	3.3	..	1	39	26.7	3	2.1	7	4.8
Brooklyn	76	82.2	12	13.0	8	4	104	24.3	13	3.1	10	2.3
Queens	15	87.7	1	5.8	..	1	21	23.4	1	1.1	4	4.5
Richmond	4	88.9	..	....	..	..	7	34.6	..	..	..	....
City of New York	266	98.7	23	8.5	12	11	472	39.8	29	2.5	41	3.5

*Includes Small Pox, Measles, Scarlet Fever, Diphtheria and Whooping Cough.

Infectious and Contagious Diseases in Hospital.

	Willard Parker Hospital. Scarlet Fever.	Diphtheria.	Measles.	Miscel.	Total.	Riverside Hospital. Scarlet Fever.	Diphtheria.	Measles.	Tuberculosis	Miscel.	Total.	Kingston Ave. Hospital. Scarlet Fever.	Diphtheria.	Measles.	Small-pox.	Miscel.	Total.	Otisville Sanatorium. Tuberculosis Pulmonalis.
Remaining Jan. 23, 1915	175	102	40	5	322	42	40	5	253	2	342	74	78	32	..	19	203	570
Admitted	34	47	10	1	92	11	13	4	4	..	32	38	31	5	..	8	82	10
Discharged	17	26	12	1	56	3	12	1	5	..	21	7	21	2	..	6	36	12
Died	3	6	1	..	10	..	..	..	1	..	4	2	..	..	..	1	6	..
Remaining Jan. 30, 1915	189	117	37	5	348	50	38	8	251	2	349	103	85	35	..	20	243	568
Total treated	209	149	50	6	414	53	53	9	257	2	374	112	109	37	..	27	285	580

51

Figure S22: Weekly Bulletins Vol 1: Sample Page from 1915.

THE HEALTH DEPARTMENT'S BABY SAVING WORK.

In 1876, owing to an unusually high mortality occurring in infants, the Department of Health obtained a special appropriation for the employment of a staff of physicians during the months of July and August. This staff was known as the "Summer Corps," and the physicians were required to canvass the tenements in the most congested quarters of the City. They treated all sick babies found whose parents were otherwise unable to obtain medical care. This plan was followed each summer for many years.

That it achieved results in the reduction of infant mortality is shown by the decrease in the number of infant deaths during this period, but its efficiency was limited in that the system was directed toward treating sick babies and not primarily toward the prevention of illness.

In 1902 seventeen trained nurses were added to the staff, and were assigned to duty in the work of school medical inspection during the school term, assisting the inspectors of the summer corps during July and August. These nurses instructed mothers in the methods of preparing food for babies, as well as demonstrating proper methods of bathing, clothing, and airing. They also nursed sick babies under the care of the medical inspectors.

With the formation of the Division of Child Hygiene, under the direction of Dr. S. Josephine Baker, in the fall of 1908, a definite and constructive change was made in the department's attitude with regard to the best means to be used in effecting a definite reduction in the infant death rate. The appointment of a staff of 141 nurses for the medical inspection of school children afforded an opportunity of employing these nurses to instruct mothers in proper baby care, not only during the summer months, but also in connection with their school duties during the early spring.

Milk Stations Established in 1911.

In 1911 the desire to treat infant mortality as a year-round problem, and to carry out more effectively the policy of preventing disease among babies, was made practically possible by an added appropriation of $40,000 for the purpose of establishing fifteen infants' milk stations. In addition, the Bureau changed its system of home visiting of babies so as to insure more revisits in each case.

Owing to the successful results obtained in the reduction of infant mortality during 1911, the Department of Health received an added appropriation for 1912 sufficient to establish forty (40) additional infants' milk stations.

For 1916 the Department received an additional appropriation allowing for the establishment of four more stations, making a total of fifty-nine now maintained under its supervision. Some idea of the magnitude of the work performed by the milk stations may be gained from the fact that during 1915 over 46,000 new cases were registered at the Health Department's Stations, the mothers making a total of 1,182,286 visits to the stations. In addition to these, 273,000 home visits were made by physicians, nurses and nurses' assistants.

Cases of Infectious and Contagious Diseases Reported.

Week Ending	Feb. 5	Feb. 12	Feb. 19	Feb. 26	Mar. 4	Mar. 11	Mar. 18	Mar. 25	Apr. 1	Apr. 8	Apr. 15	Apr. 22	Apr. 29
Tuberculosis	428	388	428	378	546	456	351	364	385	415	466	409	450
Diphtheria and Croup	372	328	391	300	316	342	264	347	312	304	373	313	302
Measles	345	308	559	503	527	576	696	772	939	932	1,045	1,019	1,095
Scarlet Fever	188	154	175	173	179	190	208	226	234	194	214	224	177
Chickenpox	171	220	194	208	273	259	304	320	398	430	440	279	404
Typhus Fever	...	...	...	...	..	...	...	1	...	1	...	...	...
Typhoid Fever	18	13	21	10	18	12	17	17	20	20	34	32	13
Whooping Cough	104	121	112	143	166	180	169	203	245	268	270	259	280
Syphilis	382	309	350	363	425	305	350	330	547	391	373	372	439
Gonorrhoea	134	100	141	90	178	64	76	73	330	65	108	93	249

150

Figure S23: Weekly Bulletins Vol 2: Only Relevant Data Page

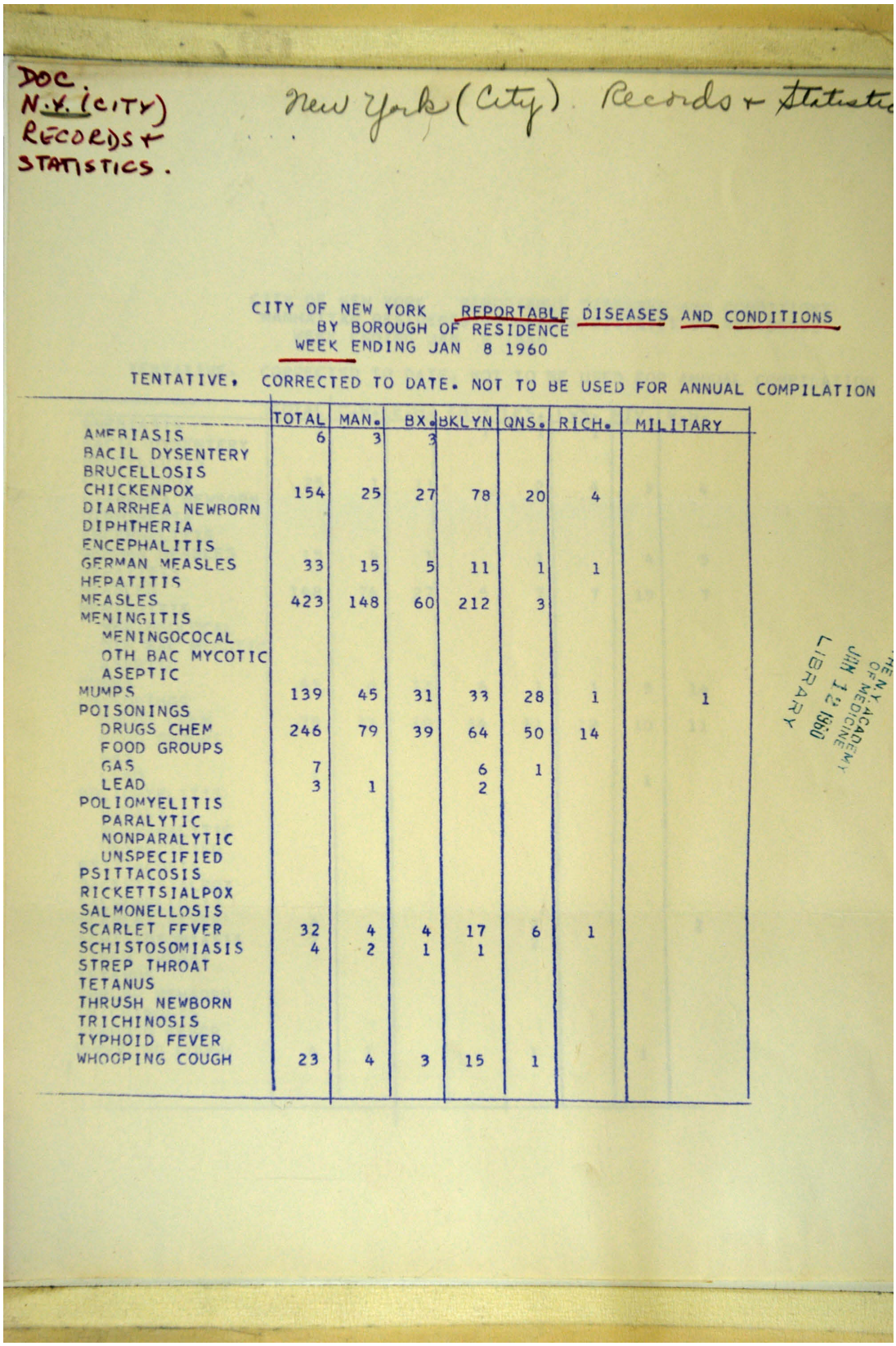

DOC
N.Y. (CITY)
RECORDS +
STATISTICS.

New York (City). Records + Statistic

CITY OF NEW YORK REPORTABLE DISEASES AND CONDITIONS
BY BOROUGH OF RESIDENCE
WEEK ENDING JAN 8 1960

TENTATIVE, CORRECTED TO DATE. NOT TO BE USED FOR ANNUAL COMPILATION

	TOTAL	MAN.	BX.	BKLYN	QNS.	RICH.	MILITARY
AMEBIASIS	6	3	3				
BACIL DYSENTERY							
BRUCELLOSIS							
CHICKENPOX	154	25	27	78	20	4	
DIARRHEA NEWBORN							
DIPHTHERIA							
ENCEPHALITIS							
GERMAN MEASLES	33	15	5	11	1	1	
HEPATITIS							
MEASLES	423	148	60	212	3		
MENINGITIS							
MENINGOCOCAL							
OTH BAC MYCOTIC							
ASEPTIC							
MUMPS	139	45	31	33	28	1	1
POISONINGS							
DRUGS CHEM	246	79	39	64	50	14	
FOOD GROUPS							
GAS	7			6	1		
LEAD	3	1		2			
POLIOMYELITIS							
PARALYTIC							
NONPARALYTIC							
UNSPECIFIED							
PSITTACOSIS							
RICKETTSIALPOX							
SALMONELLOSIS							
SCARLET FEVER	32	4	4	17	6	1	
SCHISTOSOMIASIS	4	2	1	1			
STREP THROAT							
TETANUS							
THRUSH NEWBORN							
TRICHINOSIS							
TYPHOID FEVER							
WHOOPING COUGH	23	4	3	15	1		

Figure S24: Health Department Records: Page 1

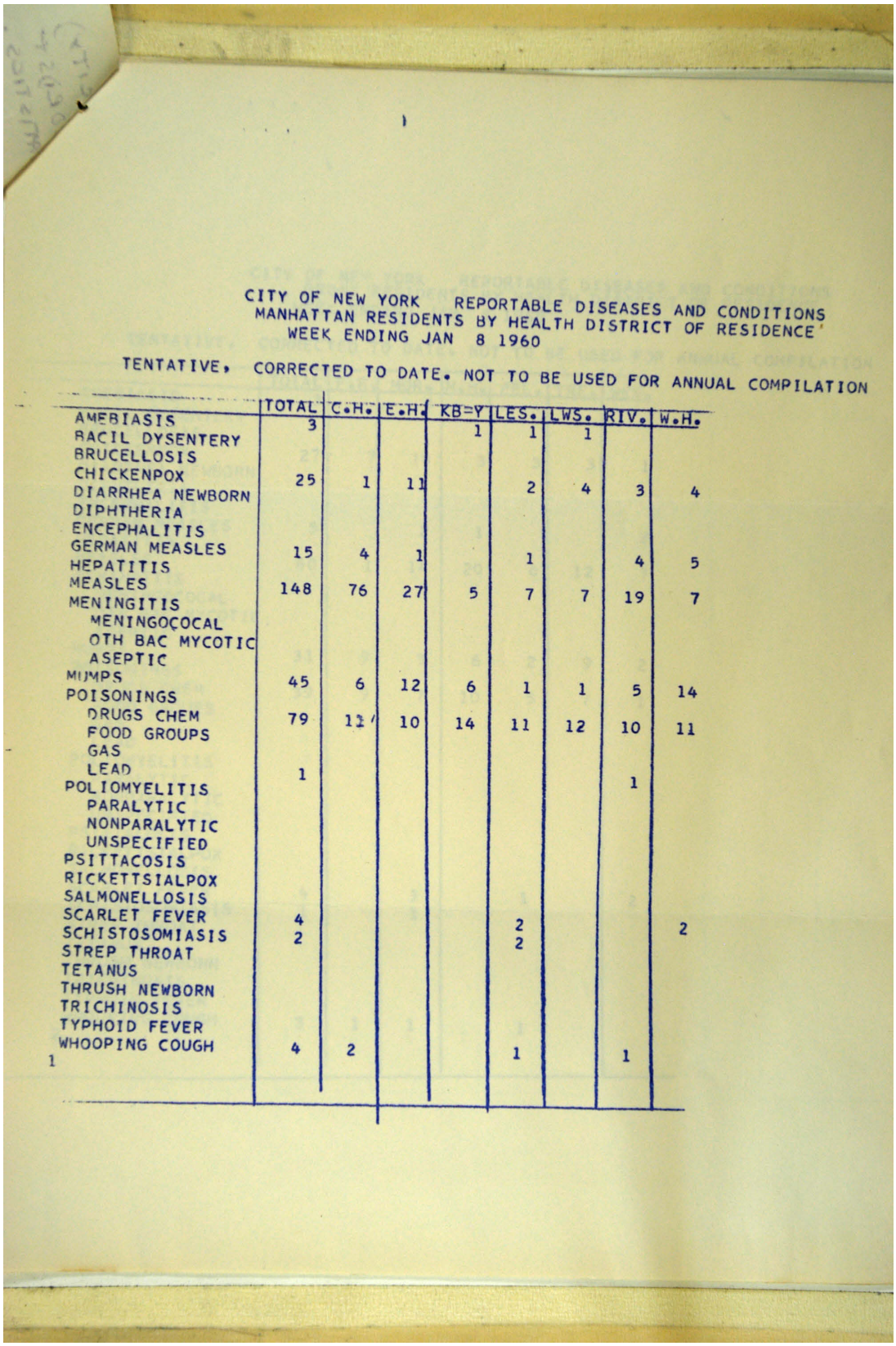

CITY OF NEW YORK REPORTABLE DISEASES AND CONDITIONS
MANHATTAN RESIDENTS BY HEALTH DISTRICT OF RESIDENCE
WEEK ENDING JAN 8 1960

TENTATIVE. CORRECTED TO DATE. NOT TO BE USED FOR ANNUAL COMPILATION

	TOTAL	C.H.	E.H.	KB=Y	LES.	LWS.	RIV.	W.H.
AMEBIASIS	3			1	1	1		
BACIL DYSENTERY								
BRUCELLOSIS								
CHICKENPOX	25	1	11		2	4	3	4
DIARRHEA NEWBORN								
DIPHTHERIA								
ENCEPHALITIS								
GERMAN MEASLES	15	4	1		1		4	5
HEPATITIS								
MEASLES	148	76	27	5	7	7	19	7
MENINGITIS								
MENINGOCOCAL								
OTH BAC MYCOTIC								
ASEPTIC								
MUMPS	45	6	12	6	1	1	5	14
POISONINGS								
DRUGS CHEM	79	11	10	14	11	12	10	11
FOOD GROUPS								
GAS								
LEAD	1						1	
POLIOMYELITIS								
PARALYTIC								
NONPARALYTIC								
UNSPECIFIED								
PSITTACOSIS								
RICKETTSIALPOX								
SALMONELLOSIS								
SCARLET FEVER	4				2			2
SCHISTOSOMIASIS	2				2			
STREP THROAT								
TETANUS								
THRUSH NEWBORN								
TRICHINOSIS								
TYPHOID FEVER								
WHOOPING COUGH	4	2			1		1	

Figure S25: Health Department Records: Page 2

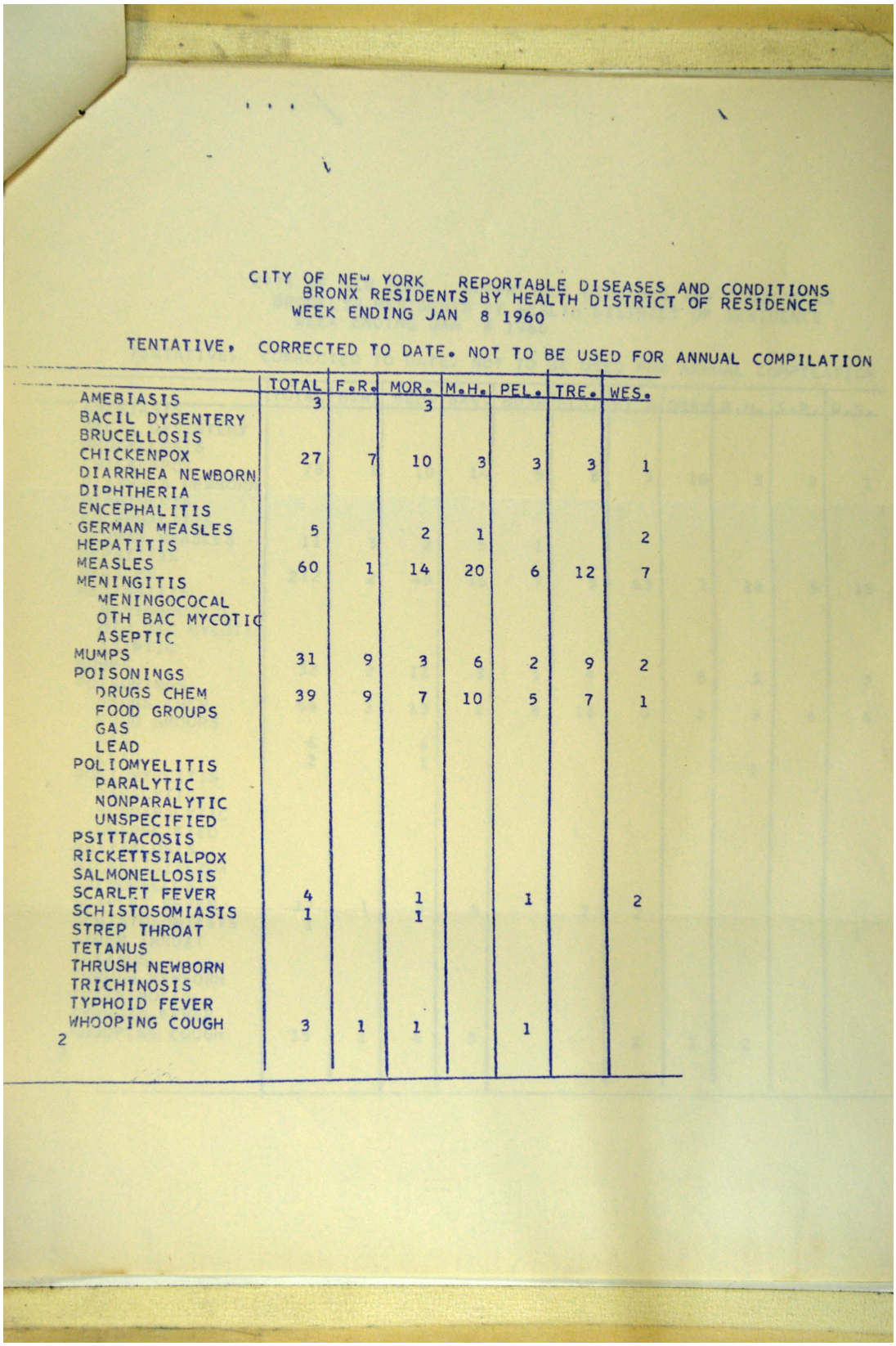

CITY OF NEW YORK REPORTABLE DISEASES AND CONDITIONS
BRONX RESIDENTS BY HEALTH DISTRICT OF RESIDENCE
WEEK ENDING JAN 8 1960

TENTATIVE, CORRECTED TO DATE. NOT TO BE USED FOR ANNUAL COMPILATION

	TOTAL	F.R.	MOR.	M.H.	PEL.	TRE.	WES.
AMEBIASIS	3		3				
BACIL DYSENTERY							
BRUCELLOSIS							
CHICKENPOX	27	7	10	3	3	3	1
DIARRHEA NEWBORN							
DIPHTHERIA							
ENCEPHALITIS							
GERMAN MEASLES	5		2	1			2
HEPATITIS							
MEASLES	60	1	14	20	6	12	7
MENINGITIS							
MENINGOCOCAL							
OTH BAC MYCOTIC							
ASEPTIC							
MUMPS	31	9	3	6	2	9	2
POISONINGS							
DRUGS CHEM	39	9	7	10	5	7	1
FOOD GROUPS							
GAS							
LEAD							
POLIOMYELITIS							
PARALYTIC							
NONPARALYTIC							
UNSPECIFIED							
PSITTACOSIS							
RICKETTSIALPOX							
SALMONELLOSIS							
SCARLET FEVER	4		1		1		2
SCHISTOSOMIASIS	1		1				
STREP THROAT							
TETANUS							
THRUSH NEWBORN							
TRICHINOSIS							
TYPHOID FEVER							
WHOOPING COUGH	3	1	1		1		

2

Figure S26: Health Department Records: Page 3

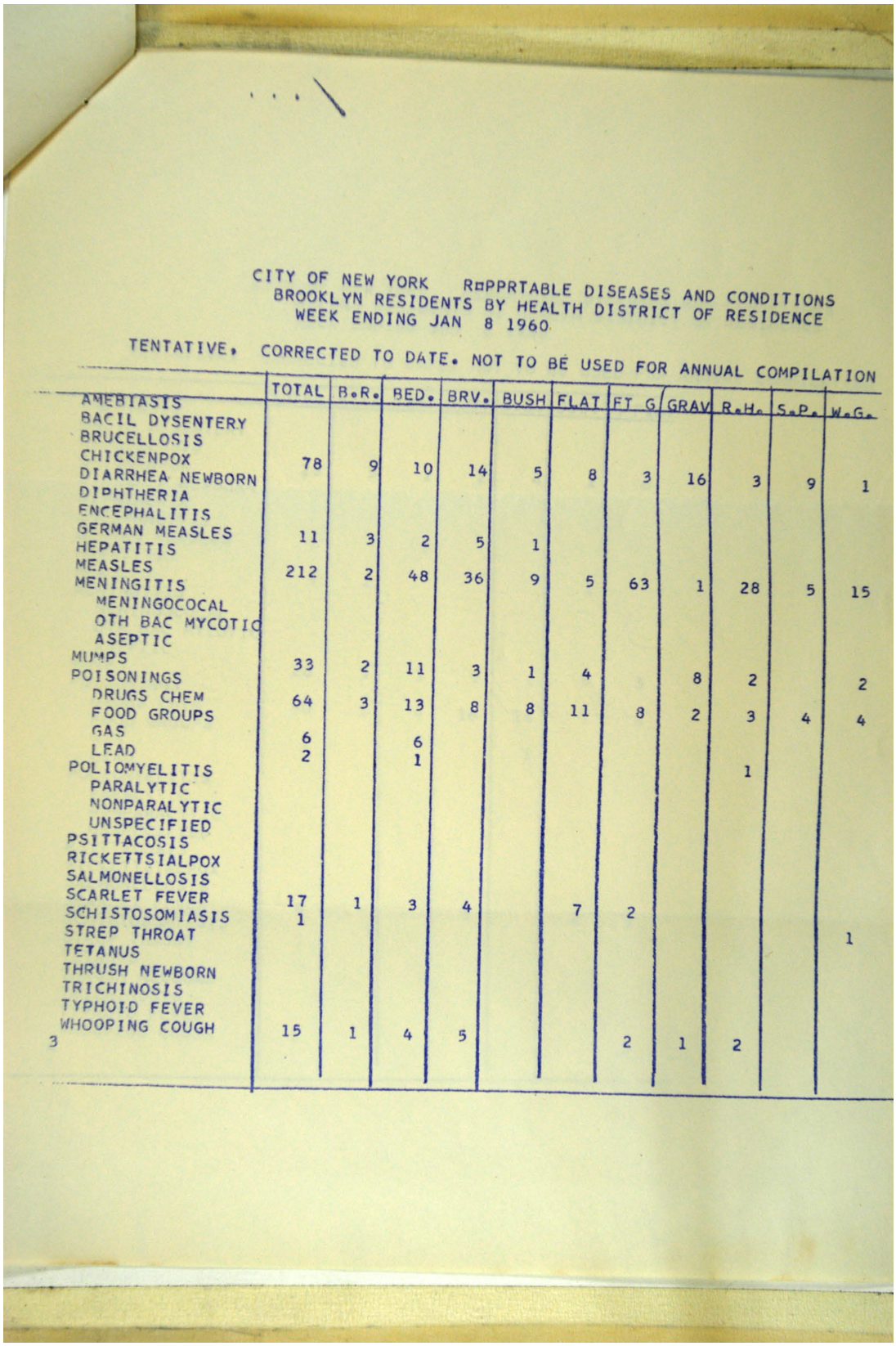

CITY OF NEW YORK REPORTABLE DISEASES AND CONDITIONS
BROOKLYN RESIDENTS BY HEALTH DISTRICT OF RESIDENCE
WEEK ENDING JAN 8 1960

TENTATIVE, CORRECTED TO DATE. NOT TO BE USED FOR ANNUAL COMPILATION

	TOTAL	B.R.	BED.	BRV.	BUSH	FLAT	FT G	GRAV	R.H.	S.P.	W.G.
AMEBIASIS											
BACIL DYSENTERY											
BRUCELLOSIS											
CHICKENPOX	78	9	10	14	5	8	3	16	3	9	1
DIARRHEA NEWBORN											
DIPHTHERIA											
ENCEPHALITIS											
GERMAN MEASLES	11	3	2	5	1						
HEPATITIS											
MEASLES	212	2	48	36	9	5	63	1	28	5	15
MENINGITIS											
MENINGOCOCAL											
OTH BAC MYCOTIC											
ASEPTIC											
MUMPS	33	2	11	3	1	4		8	2		2
POISONINGS											
DRUGS CHEM	64	3	13	8	8	11	8	2	3	4	4
FOOD GROUPS											
GAS	6		6								
LEAD	2		1						1		
POLIOMYELITIS											
PARALYTIC											
NONPARALYTIC											
UNSPECIFIED											
PSITTACOSIS											
RICKETTSIALPOX											
SALMONELLOSIS											
SCARLET FEVER	17	1	3	4		7	2				
SCHISTOSOMIASIS	1										
STREP THROAT											1
TETANUS											
THRUSH NEWBORN											
TRICHINOSIS											
TYPHOID FEVER											
WHOOPING COUGH	15	1	4	5			2	1	2		

3

Figure S27: Health Department Records: Page 4

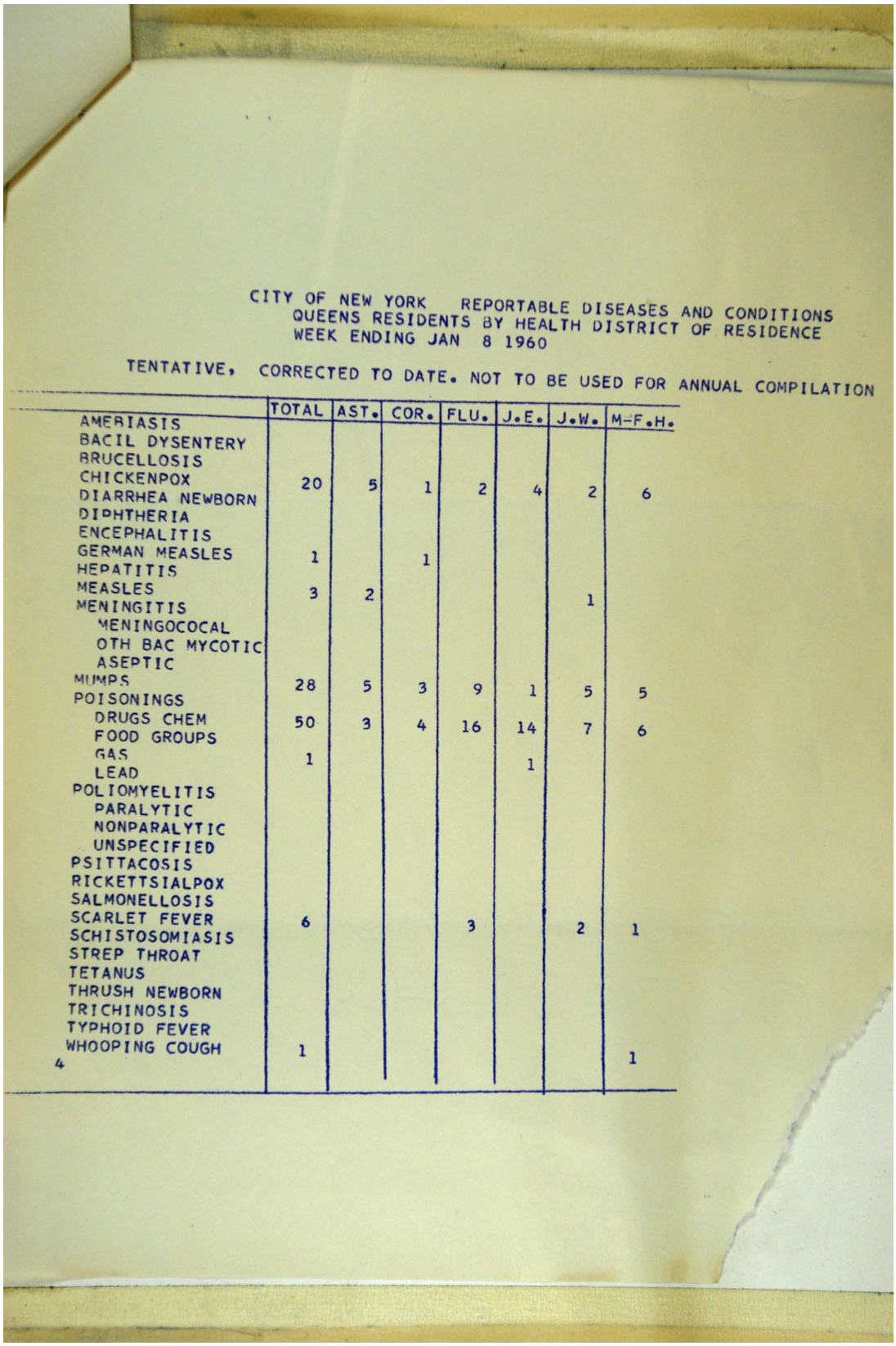

CITY OF NEW YORK REPORTABLE DISEASES AND CONDITIONS
QUEENS RESIDENTS BY HEALTH DISTRICT OF RESIDENCE
WEEK ENDING JAN 8 1960

TENTATIVE, CORRECTED TO DATE. NOT TO BE USED FOR ANNUAL COMPILATION

	TOTAL	AST.	COR.	FLU.	J.E.	J.W.	M-F.H.
AMEBIASIS							
BACIL DYSENTERY							
BRUCELLOSIS							
CHICKENPOX	20	5	1	2	4	2	6
DIARRHEA NEWBORN							
DIPHTHERIA							
ENCEPHALITIS							
GERMAN MEASLES	1		1				
HEPATITIS							
MEASLES	3	2				1	
MENINGITIS							
MENINGOCOCAL							
OTH BAC MYCOTIC							
ASEPTIC							
MUMPS	28	5	3	9	1	5	5
POISONINGS							
DRUGS CHEM	50	3	4	16	14	7	6
FOOD GROUPS							
GAS	1				1		
LEAD							
POLIOMYELITIS							
PARALYTIC							
NONPARALYTIC							
UNSPECIFIED							
PSITTACOSIS							
RICKETTSIALPOX							
SALMONELLOSIS							
SCARLET FEVER	6			3		2	1
SCHISTOSOMIASIS							
STREP THROAT							
TETANUS							
THRUSH NEWBORN							
TRICHINOSIS							
TYPHOID FEVER							
WHOOPING COUGH	1						1

4

Figure S28: Health Department Records: Page 5

References

1 New York Academy of Medicine. 1216 5th Avenue, New York, NY 10029, United States. www.nyam.org.

2 New York City Department of Health and Mental Hygiene, Office of Vital Records. Summary of Vital Statistcs, 1961-2007 Archived Reports. Available from: http://www.nyc.gov/html/doh/html/vr/vr-archives.shtml.

3 C. T. Bauch and D. J. D. Earn. Transients and attractors in epidemics. *Proceedings of the Royal Society of London, Series* B, 270(1524):1573–1578, 2003.

4 Peter H Baxendale and Priscilla E Greenwood. Sustained oscillations for density dependent Markov processes. *Journal of Mathematical Biology*, 63(3):433–457, 2011.

5 B. Cazelles, M. Chavez, G. C. de Magny, J. F. Guegan, and S. Hales. Time-dependent spectral analysis of epidemiological time-series with wavelets. *Journal Of The Royal Society Interface*, 4(15):625–636, 2007.

6 Bernard Cazelles, Mario Chavez, Dominique Berteaux, Frédéric Ménard, Jon Olav Vik, Stéphanie Jenouvrier, and Nils C Stenseth. Wavelet analysis of ecological time series. *Oecologia*, 156(2):287–304, 2008.

7 D. J. D. Earn. Mathematical epidemiology of infectious diseases. In M. A. Lewis, M. A. J. Chaplain, J. P. Keener, and P. K. Maini, editors, *Mathematical Biology*, volume 14 of *IAS/ Park City Mathematics Series*, pages 151–186. American Mathematical Society, 2009.

8 D. He and D. J. D. Earn. Epidemiological effects of seasonal oscillations in birth rates. *Theoretical Population Biology*, 72:274–291, 2007.

9 A. M. Holdsworth, N. K. R. Kevlahan, and D. J. D. Earn. Multifractal signatures of infectious diseases. *Journal of the Royal Society Interface*, 9(74):2167–2180, 2012.

10 Michael A Johansson, Derek A T Cummings, and Gregory E Glass. Multiyear climate variability and dengue—el nino southern oscillation, weather, and dengue incidence in puerto rico, mexico, and thailand: a longitudinal data analysis. *PLoS Medicine*, 6(11):e1000168, 2009.

11 W. London and J. A. Yorke. Recurrent outbreaks of measles, chickenpox and mumps. I. seasonal variation in contact rates. *American Journal of Epidemiology*, 98(6):453–468, 1973.

12 C. Torrence and G. P. Compo. A practical guide to wavelet analysis. *Bulletin of American Meteorological Society*, 79(1):61–78. http://atoc.colorado.edu/research/wavelets/, 1998.